A COMPARATIVE STUDY AMONG DIFFERENT CRYOPROBE CONFIGURATIONS FOR EFFECTIVE NECROSIS OF BIOLOGICAL TISSUE

B.Siva Kumar

A COMPARATIVE STUDY AMONG DIFFERENT CRYOPROBE CONFIGURATIONS FOR EFFECTIVE NECROSIS OF BIOLOGICAL TISSUE

Thesis submitted to the
National Institute of Technology, Rourkela
for the award of the degree

of

Master's of Technology in Mechanical Engineering

by

Bathina Siva Kumar

213ME5445

Under the guidance of

Dr. Amitesh Kumar

DEPARTMENT OF MECHANICAL ENGINEERING

NATIONAL INSTITUTE OF TECHNOLOGY, ROURKELA

JUNE 2015

CERTIFICATE

This is to certify that the thesis entitled **A Comparative Study Among Different Cryoprobe Configurations For Effective Necrosis of Biological Tissue**, submitted by **Bathina Siva Kumar** to National Institute of Technology, Rourkela, is an authentic record of bona fide research work carried under my supervision and I consider it worthy of consideration for the award of the degree of Master's of Technology of the Institute.

Date :

Dr. Amitesh Kumar
Assisstant Professor
Department of Biotechnology & Medical Engineering
National Institute of Technology
Rourkela, 769008

DECLARATION

I certify that

1. The work contained in the thesis is original and has been done by myself under the general supervision of my supervisor.
2. The work has not been submitted to any other Institute for any degree or diploma.
3. I have followed the guidelines provided by the Institute in writing the thesis.
4. Whenever I have used materials (data, theoretical analysis, and text) from other sources, I have given due credit to them by citing them in the text of the thesis and giving their details in the references.

B.Siva Kumar

CURRICULUM VITA

Name: Bathina Siva Kumar

Educational Qualification:

Year	Degree	Subject	University
2011	B.Tech	Mechanical Engineering	JNTU Kakinada

ACKNOWLEDGEMENTS

We dream, we desire, we strive to achieve our dreams, at last it is our perseverance and determination that pays and then only we achieve what we dream. So, today it is my dream that I am at the meridian of achieving my goal. As I begin to write these lines; after completion of my thesis, my heart is filled with deepest sense of gratitude. I shall ever remain thankfully indebted to all those who have directly or indirectly encouraged me to achieve my goal and enlightened me with the touch of their cognizance and encouragement.

First and foremost, I consider it as a blessing to pursue my project under the able guidance of Dr. Amitesh Kumar, whose insights and approvals have contributed so much to this thesis. No words are enough to express my gratitude to my mentor for his whole hearted, unflinching encouragement, meticulous supervision and support. He would take a great concern in troubleshooting problems and was always full of encouraging words. His words of applause and sincere criticism in the last one year helped me a lot to develop my ideas regarding many important issues in life.

No task is difficult if you have a friends like Prasad, Vishnu, Laxman, Keshab, Manoj who were the greatest help I could have dreamt of. They provided such a wonderful company and made my stay in N.I.T Rourkela a pleasant experience. We had such memorable time in this institute that it is painful to note that we will be moving to new places. Thanks a million, for being with me, whenever I needed any help. I will remember the wonderful time we had for a long time to come.

Where emotions are involved words cease to mean, lexicon could not have the words to express the affection, blessings, encouragement, sacrifice and love of my beloved Mother, Father, and Sister without which I would have never come to this proliferative stage and engaged myself in career building. Last and above all, having such a wonderful family that supports me whole heartedly, no matter what I do, is something I feel unique to my life. There are no words to pay regards to them for toiling so hard to bring me up to this stage.

At last, I would like to express my deep sense of gratitude to almighty GOD, many known and unknown hands which pushed me forward.

Date :
Place :

B.Siva Kumar

Contents

List of Figures

List of Tables

LIST OF SYMBOLS AND ABBREVIATIONS

c	specific heat (J/kg K)
H	specific total enthalpy (J/kg)
h	specific sensible enthalpy (J/kg)
k	thermal conductivity (W/m K)
L	specific latent heat of fusion (J/kg)
$\dot{Q}_m$	metabolic heat generation (W)
Ste	Stefan number
T	temperature (K)
t	time (s)
$\dot{m}_b$	blood perfusion rate (kg blood per m^3 of tissue per second)

Subscript

b	blood
f	frozen tissue
l	point at which freezing starts
p	probe
s	point at which freezing ends
u	unfrozen tissue

ABSTRACT

The complete necrosis of malignant biological tissue can be achieved, when the optimal parameters (generation of ice ball around the cryoprobe, ablation ratio, cooling power requirement) are known to the cryo surgeon. In this study the optimal parameters (volume of ice ball around the cryoprobe, ablation ratio, cooling power requirements) are predicted and compared to maximise the tissue necrosis. Surgical parameters like lethal zone, frozen zone and ablation ratio are studied for different placements of cryoprobes. The percentage increase in ice ball volume (obtained at the end of freezing cycle, i.e. 10 min considering with and without central cryoprobe configurations) decreases with increase in the number of offset cryoprobe at same opereating conditions. It was observed that with the increase in offset cryoprobes, there was no remarkable growth on ablation ratio at the end of freezing process. However, the less number of offset cryoprobes resulted in effective ablation during the early stage of freezing process. Also, the cooling power requirement increases with increase in the number of offset cryoprobes and also increases with decrease in cryoprobe temperature.

Keywords: Cryosurgery, Multiprobe, frozen and lethal zone, iceball volume, Ablation ratio, Cooling power, necrosis.

CHAPTER 1

Introduction

Cryosurgery, likewise alluded as cryo treatment or cryo removal, is a novel surgical procedure which utilizes compelling solidifying to obliterate unhealthy tissue . Present day time of cryosurgery started with the improvement of computerized cryo surgical hardware in the 1960s. Utilizing solidifying as the intends to pulverize undesirable tissues, cutting edge cryosurgery presents numerous surprising merits over its aggressive modalities. Cryosurgery is led by method for a cryoprobe either by putting its constantly cooled tip on or into the tissue to be solidified. Cryogens (utilized as a cooling medium)

which have been utilized as a part of cryosurgery incorporate fluid nitrogen, nitrogen oxide, strong carbon dioxide, fluid argon having bubbling temperature of $-196^{O}C$, $-89.5^{O}C$,$-78.5^{O}C$,$-187^{O}C$ separately [1]. By and large fluid nitrogen is utilized for cryogen on account of least bubbling temperature. Cryosurgery is broadly connected in the treatment of different undesired harmful and non-carcinogenic tissues in liver, lung, kidney, prostrate, cerebrum, skin, bosom, bone and so on. One of the key point of preference of cryosurgery is that cell pulverization is confined which minimizes harm to encompassing sound tissue [2]. The objective of this surgical system is to expand the annihilation of target tissue while minimizing the harm to encompassing solid tissue. Two components of tissue damage, prompt and deferred, are connected with cryosurgery. The prompt pulverization includes direct obliteration of cells while the deferred conjures post application harm because of the obliteration of veins or deferred invulnerable framework [1, 3] The essential strategy obliges quick solidifying to deadly temperature of tissue, moderate defrosting, and reiteration of the stop defrost cycle. Ice-front's positions, holding time span, stop defrost cycles, solidifying rate and instigated warm push ought to be legitimately checked for the ideal demolition of undesired tissue. The cryosurgeon screens the solidifying process by method for restorative imaging, for ex-

ample, ultrasound or MRI and conforms the cooling force of the person cryoprobe appropriately to augment the cell passing and minimize the pulverization of encompassing typical tissue or organ.

With the end goal of cryosurgical arranging, it is very attractive to register the procedure of ice spread and warm history inside the ice-ball, which can't be controlled by imaging. Mechanized arranging helps specialists in preplanning of surgery. To focus the impact of cooling rate, introduction of cryoprobe temperature, stop defrost cycle and game plan of cryoprobe on the debasement of destructive cells and warm history inside of the tumor, numerical recreations can be profitable help. Such an apparatus resounds well with specialists, furnishing them with the ability to boost the viability of the surgery. Numerical recreation can turn out to be more beneficial progressively operation to anticipate the inward warm history of the objective tissue.

1.1 Mechanism of cryosurgery

The destructive effect of freezing tissue has been categorized into two major mechanisms, one immediate and the other delayed. The immediate destruction is due to the direct destruction of cells while the delayed invokes post application damage due to the destruction of blood vessels or delayed immune system. The immediate process involves formation of intracellular and extracellular ice- crystals. As tissue temperature falls below zero degree, ice- crystals form in extracellular space and in microvasculature; this removes water from biological system and invokes hyperosmotic drying of the tissue, further tissue ablation starts. Higher rate of freezing produces intracellular ice crystals which causes progressive cell destruction [1, 3, 4, 5]. Delayed mechanism is operative during thawing. The cryogen circulation is stopped for certain time duration which causes the failure of microcirculation. Less cryogenic harm produces insufficient tissue demolition while more cryogenic damage may stretch out harmful impacts to encompassing typical tissue. For ideal cryoablation of the infected tissue, it is important to be concerned on taking after controlling parameters:

1. **Cooling rate:** In cryosurgery, quick cooling rate i.e. more than$-50^{O}C/min$ produces intracellular ice- gems which is more dangerous. Survey of trial information proposed that cooling rates of $-3^{o}C/min$, $-22^{o}C/min$ and $-50^{O}C/min$ are needed so as to affect intracellular ice in neoplastic cells, liver also, dunning AT-Tumor [3]. Such higher rates of cooling must be accomplished near to the cryoprobe and further away it brings down, and entire tissue is not subjected to quick cooling. Farrant, Walter and Mazur bolster that cooling rate is not a prime variable for cryosurgery. They recommended that the cells are presented to assorted warm profiles for diverse times [3, 6, 7, 8].

2. **Temperature:** Cryosurgical treatment obliges that deadly tissue temperature ought to be accomplished in all parts (entire) of the tumor. The lethality of solidifying increments as temperature falls an increasing amount. Mazur expressed that the deadly temperature extent is between -5^oC to -50^OC [7]. As per Cooper, -20^OC temperature for 1 min time span is adequate to create corruption [9]. Rivoire et al. [10] discovered -15^OC temperature is expected to create complete corruption. In trial with rodent liver, Smith and Fraser recommended that necrotic impact enacts at -15^OC, yet they moreover watched that some undesired cell survival was conceivable at this temperature [3, 11, 12]. The treatment of tumor obliges a tissue temperature at which all the irregular cells are positively dead. It demonstrates the significance of deadly tissue temperature in cryosurgery, particularly for the treatment of malignancy. Because of varieties in affectability and thermophysical properties of ordinary and destructive tissue, it is difficult to achieve the lethal temperature of the ailing tissue. From the survey of all test studies the end point temperature beneath -40^OC has been viewed as prime element for tissue obliteration [3, 12].

3. **Freezing duration:** a measure of ideal solidifying length of time, i.e. to what extent tissue ought to be held in a solidified state, is not known before the surgery. Mazur expressed that the rate of cell passing is most noteworthy when tissue is held at temperature above than -30^OC [6]. Underneath that temperature, little water stays unfrozen,so term is less critical. In any case, other cryosurgical examinations demonstrated its significance. Prolongation of solidifying was thought to be invaluable in trials with bosom tumors in creatures. Longer solidifying likewise created more harm to the ligament of the ears of pigs. Gage and Baust recommended that stop length of time is immaterial if the tissue is held at temperatures colder than -50^OC, however holding tissue at hotter temperature i.e. more than -40^OC, will increment damaging impact.

4. **Thawing rate:** Defrosting rate ought to be moderate and proceeded for more time period; quick defrost rates permit cell survival. Inside of temperature scope of -20^OC to -25^OC, defrost is more critical because of maximal development of ice-precious stones. On the off chance that tissue is held at this temperature for more span, cell passing is more powerful because of recrystallization procedure which delivers extensive ice precious stones. Prolongation of defrost is profitable in cell harm just on the off chance that it is handled totally [2, 3, 8].

5. **Repetitive freeze-thaw cycles**: Fast solidifying and moderate defrosting don't promise powerful cell devastation. Accordingly, the cryosurgery procedure ought to be customized in such an approach to create suitable deadly impact to certain volume

of tissue. Presently stop defrost cycle came into idea, each of which cycle is harmful to cells [2]. Amid reiteration of cycles, a few times cells experience through irritated warm conditions than the warm conditions for their survivability, this prompts more volume of cell demise. Stop defrost cycle is more damaging if redundancy is performed inside of temperature scope of $-20^{O}C$ to $-30^{O}C$. Intracellular ice development is dynamic in rehashed cycles, which reasons tissue scraped area. Utilization of rehashed stop defrost cycle is likewise helpful in treatment of malignant tumor [3, 12].

1.2 Monitoring cryosurgery

Disgraceful observing of cryosurgical procedure may prompt either inadequate surgery or an extra undesired harm to sound tissue. Accordingly, for ideal decimation of unhealthy item, checking ought to be performed absolutely and all the while degree of solidifying ought to be assessed. There are taking after methods for cryosurgery checking.

1.2.1 Local monitoring technique

Nearby checking strategies are taking into account thermometry and impedancemetry. In first case, thermocouples are embedded inside the tissue to be solidified for direct estimation of nearby temperature and in second case terminal needles are put inside the objective tissue to recognize solidifying actuated changes in nearby impedance. While thermometry and impedancemetry have a significant commitment to cryosurgery, they likewise have some real disadvantages. Both are intrusive also, have restricted warm data (just for embedded site) [13]. Subsequently, absence of definite information may forward to blame result.

1.2.2 Image monitoring technique

In cryosurgery, ultrasound was the first imaging method utilized as a part of clinical cryosurgery on the grounds that it was less demanding to utilize and conservative. A few systems are accessible for acoustic imaging of the body. A short beat of electrical vitality is changed over into a burst of acoustic vitality with a piezoelectric transducer. The weight wave that is delivered engenders through the body. At the point when the weight heartbeat experiences the limit between areas with diverse acoustic impedance,part of the wave is reflected back to the transducer where it is changed over back to an electrical motivation. The piezoelectric transducer capacities both as an emitter and a finder. In entire body imaging it is accepted that the speed of the acoustic wave is pretty nearly 1450 m/s. At the point when weight waves come back to the piezoelectric component, the deliberate time of flight of these wave output be joined with learning of the tissue

wave pace to focus the area of the acoustic impedance irregularity. Two-dimensional pictures of acoustic discontinuities in tissue can be delivered utilizing numerous piezo-electric components and PC investigation of the information. The precision of ultrasound pictures is restricted by the presumption of the wave speed in tissue.Freezing interfaces can be helpfully checked with customary ultrasound on the grounds that there is an expansive distinction in acoustic impedance in the middle of ice and water. Ice basically mirrors all the acoustic vitality, subsequently whole solidifying region looks dull.

Ultrasound can just catch the picture of the solidifying interface before transducer, this is the issue connected with ultrasound.Magnetic reverberation imaging (MRI) produces a picture of the body organ by applying a substituting attractive field. It creates a picture of proton thickness, which nearly identifies with tissue structures. X-ray delivers an exact three-dimensional picture of solidifying interface; in this way it can be utilized to figure the temperature appropriation in the solidified area. X-ray has tackled the issue experienced by ultrasound as it has the capacity deliver constant three-dimensional picture off solidified tissue without acoustic shadowing. On the other hand, high cost and exceptional surgical environment may utmost its use.

Another imaging strategy is optical checking; it beats the issue of ultrasound and is additionally less extravagant. It utilizes two strategies: one uses the season of flight of a proton through the tissue, and other is in light of diffusing attributes of the tissue. In both the techniques, light is discharged on one tissue-surface and recognized on other. Tomography is then used to remake the picture from the optical properties of the tissue. Adequate optical differentiation ought to exist to catch the continuous changes in tissue while solidifying. Electrical impedance tomography (EIT) is another new strategy that may give an reasonable and adaptable supplement to existing cryosurgical checking procedures. Infusing little sinusoidal electrical streams into the body and measuring the subsequent voltages through a terminal cluster creates a run of the mill EIT picture. An impedance picture of the tissue is then created from the voltage information utilizing a remaking calculation [13].

1.2.3 Mathematical modeling

Above imaging procedures just screen the external solidifying front and those are not ready to give warm data inside the solidified tissue. At that point scientific models started to be to foresee the warm history inside of the objective article and the degree of solidifying. In view of bio-warmth mathematical statement, warmth exchange model has been produced to portray cryosurgical process numerically. Numerous researchers have forced scientific systems to assess and advance the cryosurgical arranging. It can be utilized by specialists as a part of ongoing cryosurgery. Be that as it may, to make it

more viable there is requirement for the consideration of cutting edge numerical methods [2]

1.3 Advantages of cryosurgery over conventional surgical treatment

1. Minimal invasion of tissue
2. Less bleeding
3. Local application
4. Less time taking
5. Anesthetic capabilities
6. Repetition of procedure
7. Minimal hospitalization
8. Less expensive

1.4 Review of Literature

In the treatment of cancer, a sufficiently low temperature should be ensured so as to effect complete destruction. Mazur [7] defines the critical temperature for cell destruction within the range of $-5^{O}C$ to $-50^{O}C$. Intracellular ice forms in prostate cells at temperatures below $-40^{O}C$ [14], which, therefore, serves as a target temperature in this application. Other investigators suggest that even higher temperatures, e.g., $-20^{O}C$, may be lethal to the cells [15]. The cooling rate maintained at the freezing front has also been cited as a factor that determines the survival of the frozen tissue [16]. Cryosurgery of a biological tissue or tissue-simulating gel with one or multi-cryoprobe have been studied both experimentally and numerically by many researchers [17–20]. Consequently, investigators employ numerical solution techniques, e.g., the front tracking method [21] or the enthalpy method [22]. The application of multiprobes in tissue like substances was analysed by Keanini and Rubinsky [23] who presented a general technique for optimising cryosurgical procedures. Rewcastle et al. [18] analysed the ice ball formation using an axisymmetric, finite difference model around a single cryoprobe. Model predictions were compared to measured data and were found to conform to within $\pm 5^{o}C$. Jankun et al. [24] developed an interactive software simulation package (CRYOSIM) for cryoablation of the prostate by liquid nitrogen operated cryoprobes. The model is based on a finite difference numerical technique.

For optimisation of multiprobes, Baissalov et al. [25] discussed a semiemphrical treatment planning model. In order to analyse the 3D heat transfer problem in a model of prostate, they developed a finite element procedure. The locations of the frozen front were predicted and compared to X-ray readings within ±2mm. They considered six cryoprobes at equal radial distances from a central urethral warmer. A 3D finite difference ice ball formation for one, three and five cyroprobes was analysed by Rewcastle et al. [19]. A 3.4mm diameter argon-operated probes with 30mm long active segments yielded close comparisons to experimental data in gelatin. Assuming an ablative temperature of -40°C, it was found that the maximum ablative ratios for three and five probe configurations were 0.21 and 0.3 respectively. For the same time interval, it was found that the ablation ratio for three probe configuration was higher than the corresponding five probe configuration. A finite model of multiprobe cryosurgery of the prostate was presented by Wan et al. [26] based on a variation principle. Rabin and Shitzer [20] presented a cooling power requirement by cryoprobe for freeze cycle. For instance, the lowest cryoprobe temperature of -126^oC (Joule Thomson effect) require a power 35% lower than that required for the cryoprobe temperature(liquid Nitrogen) of -196^oC. Magalov et al. [27] studied the multiprobe configuration experimentally and numerically in which they considered the four configurations of placing three probes. They found that, the far apart placement configurations which produces the maximum volume enclosed by iceball front were always more than the other configuration. But, they found entirely opposite trend for -20^OC and -40^OC iceballs. In computerised planning of prostate cryosurgery, Rossi et al. [28] used bubble-packing method for the planning. They studied the process with multiprobe at different insertion depths. Recently, an effective finite differences method was proposed for simulation of bioheat transfer in irregular tissues by He et al. [29] and extended the alternating direction implicit finite-difference metod (ADI-FDM) algorithm to reduce the staircase effects resulting due to irregular boundary. For simulating the cryosurgery process software package ANSYS or finite difference method was used by most of the investigtors and they approximated the cylindrical cryoprobe with the cuboidal cryoprobe.

Cryosurgergy of a biological tissue with the effect of central probe was studied by Kumar.A. [30] This work is an extension to previous work. The purpose of present study is to find out the optimal cryoprobe configuration among the four, five and six offset with or without central probe to maximise the cell necrosis. The multiblock, non-orthogonal, body-fitted-grid system was taken to study a phase change problem in a complex geometry created by the presence of cryoprobes, and finite volume formulation method is used for solving the present numerical model for obtaining the discritised governing differential equation.

1.5 Outline of the thesis

Comparision among different cryoprobe configuration for effective necrosis of biological tissue is the main work of this thesis. This thesis consists of three chapters. A brief description of each chapter is given below.

Chapter 1: This chapter consists of general background of cryosurgery, mechanism of tissue freezing, monitoring techniques of cryosurgery, importance of mathematical modeling and, literature review and objective of the study.

Chapter 2: In this chapter a three-dimensional numerical model for cryosurgery is developed for comparing different cryoprobe configurations with and without central probe. The irregular boundary resulting due to the presence of cryoprobes is taken care by body-fitted multi-block non-orthogonal grids. The thermo-physical properties of biological tissue are considered as a function of temperature as phase change takes place over a wide temperature range for the biolog- ical tissue. The fundamental Pennes equation has been used to study the heat transfer during cryosurgery process. The Pennes heat transfer equation in its usual form is given. Numerical code is validated against the analytical results of one-dimensional phase change problem and three-dimensional heating of a semi-infinite slab due to a moving point source.

Chapter 3: In this chapter, the results obtained for different cryoprobe congfigurations are discussed and compared. On the basis of these results, the conclusions are drawn.

CHAPTER 2

MATHEMATICAL FORMULATION

Out and out six distinct arrangements of cryoprobe situation have been considered. Figure 2.2 demonstrates the distinctive setups concentrated on in this study. All the counterbalance tests are set at the same spiral area of 10 mm from the focal hub and they are embedded into the tissue to the same profundity of 60 mm; the dynamic length being 20 mm. Additionally, all the tests are comparative in measurement having diameter equivalent to 3 mm. At first the tissue is thought to be at uniform temperature of 370C.

2.1 The governing equation

For studying heat transfer during cryosurgery the fundamental Pennes equation is uused. The Pennes heat transfer has been taken in its usual form is given as

$$\frac{\partial(\rho H)}{\partial t} = \nabla \cdot (k \nabla T) + \dot{m}_b c_b (T_b - T) + \dot{Q}_m \tag{2.1}$$

where ρ is the density of the tissue, $H = h + \int c\, dT$, is the total specific enthalpy, h is the specific sensible enthalpy, c is the specific heat at constant pressure, $\dot{m}_b$ is the blood perfusion rate, T is the temperature, and $\dot{Q}_m$ is the metabolic heat generation rate.

The Pennes equation is similar to the general heat diffusion equation with exception of the second and the third terms appearing in the right hand side of equation 2.1. The second and third terms on the right hand side of the equation represent the internal heat sink due to blood flow and metabolism, respectively. It has been assumed that blood enters the target tissue with fixed temperature T_b. It has been observed that for a particular body mass and activity, the heat generated due to metabolic process is rel-

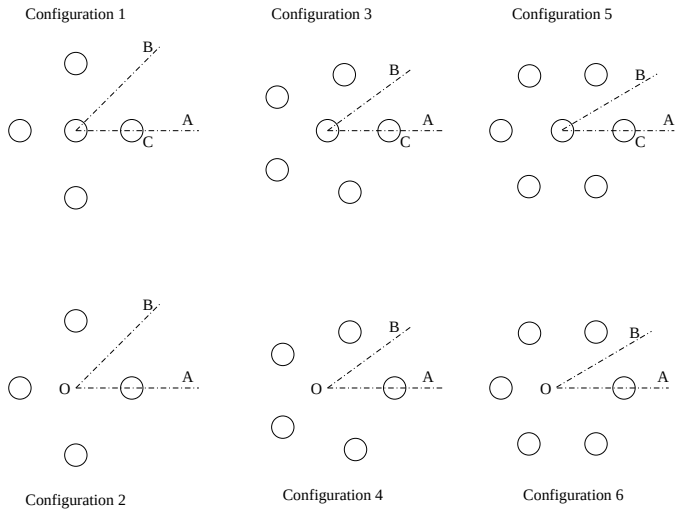

Figure 2.1: Cryoprobe placement configurations for symmetrically placed four, five, and six cryoprobes with or without a central cryoprobe

atively constant. The numerical solution of equation 2.1 is obtained for the following assumptions:

1. Heat transfer in the tissue is purely by diffuson;
2. Phase transition occurs over a wide temperature range between -0.53^oC (upper limit) and -8^oC (lower limit) [20, 31];
3. Thermal conductivity varies drastically with the temperature;
4. Blood perfusion and metabolism act as heat sink for the unfrozen tissue.

2.2 Solution approach

The three-dimensional dispersion comparison with phase change, blood perfusion, and metabolism system is discretised on an organized multiblock non-orthogonal grid system utilizing finite volume approach. In light of the symmetry of the tissue stand out one-eighth, one-tenth, and one-twelfth part of the tissue is recreated for configuration 1-2, configuration 3-4, configuration 5-6 individually. A common computational domain with grid densities at diverse pivotal areas is indicated in figure 2.2. This figure 2.2 also indicates that the presence of central probe. Diverse shades of the limit are illustrative of the distinctive pieces utilized as a part of the reproduction. The axial length is additionally demonstrated in the figure. The axial length of the computational area is taken as 100 mm while is taken equivalent to 60 mm. The aforementioned separations are discovered adequate to force the basal body temperature, 37^oC, condition at the limits of the space. It ought to be noticed that grids are laid in such a way that grid density is higher close to the extensive temperature inclination zone (i.e. close to the

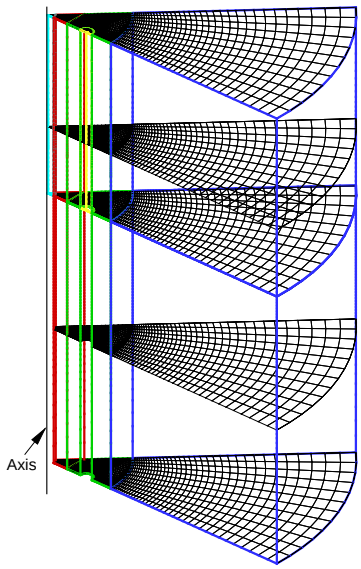

Figure 2.2: a typical computational domain

cryoprobes) also, it is lower at the limits of the area. A multiblock grid system having five blocks of 24×12×96, 36×24×96, 36×12×96, 12×12×36, and 36×12×36 control volumes is found sufficient to resolve the temperature fields and the frozen and the unfrozen fronts during the freezing process for the case of configurations with a central cryoprobe while the respective control volumes are 24×12×96, 36×24×96, 36×12×96, 12×12×96, and 36×12×36 for the case of configurations without the central cryoprobe. Case in point, figure 2.3 demonstrates the variation of ablation ratio and the cooling power with time for two arrangements of grid densities. The fine grid density relates to the aforementioned control volumes. It can be seen that with expansion in number of control volumes the adjustment in expectations is practically unimportant. The diffusive term and the precarious term are discretised utilizing central difference schemes and the implied three time level technique (a quadratic in reverse close estimation) separately offering ascent to second order accuracy in space and also in time. Definite discussion about implicit three time level plan and the structured multiblock system here can be found in Ferziger and Peric [32]. Settled network enthalpy method, because of Voller and Prakash [33], is used to take care of the phase change issue.

2.3 Code validation

The present numerical code is accepted against the expository after effects of one-dimensional stage change issue and three-dimensional warming of a semi-unbounded section because of a moving point source and the distributed trial consequence of temperature history at few focuses in a solidifying gel

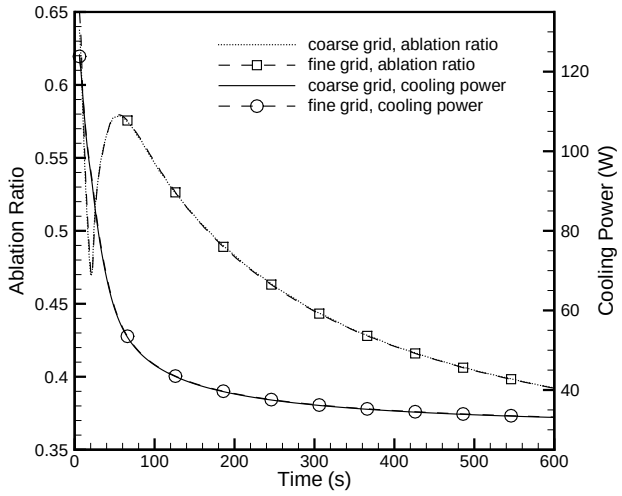

Figure 2.3: Grid independency test

2.3.1 Melting in a semi-infinite domain

A solid, $x \geq 0$, initially at the melting temperature T_m is considered for this case [34]. Surface of the solid at $x = 0$ is raised to a temperature T_w ($> T_m$) at time $t = 0$ and maintained at this constant value for times $t > 0$. Thus melting starts at the surface and the melting front moves in the positive x-direction. Being at the uniform temperature T_m throughout, there is no heat transfer in the solid phase. Only diffusion-controlled phase change with constant thermo-physical properties values have been considered for this purpose. The exact solution for the position of the melting front is given by Kakac and Yener [34]. For numerical purpose the semi-infinite domain is considered to be of finite length l_{solid}. The thermo-physical properties of the solid, T_w and T_m are chosen in such a way that Stefan number Ste = $c(T_w - T_m)/L$= 1. The numerical prediction matches quite well with the anlytical solution [35]. The above validation shows the capability of present numerical code to handle phase change phenomena precisely.

2.3.2 Three dimensional heating of a semi-infinite slab due to a moving point source

the computer code is approved against a three-dimensional logical answer for heating of a semi-infinite slab with a moving heat point source at first glance [36]. The slab is infinite in the x and y bearings. The model considered for the present issue is indicated in figure 2.4 . The point source is moving with speed -U in the -x direction (the semi-infinite slab is moving towards the heat source with U in the x course). Plane CDEF is a plane of symmetry. Heat loss from the surface by any methods is ignored. The systematic answer for quasi steady temperature distribution in the semi-infinite slab is given

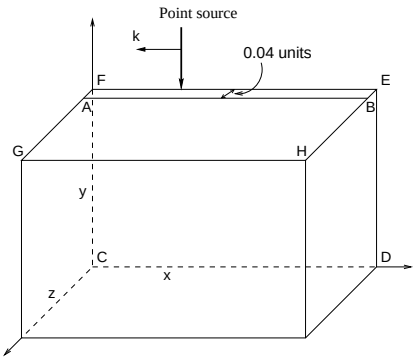

Figure 2.4: Computational model for 3-D heating of a slab

by

$$T - T_0 = \frac{P}{2\pi k r'} exp\left(U\frac{(x'-r')}{2\alpha}\right) \tag{2.2}$$

where

$$\begin{aligned} x' &= x - x_{point} \\ r' &= \sqrt{\left(x-x_{point}\right)^2 + \left(y-y_{point}\right)^2 + \left(z-z_{point}\right)^2} \end{aligned}$$

x_{point}, y_{point} and z_{point} are the x, y and z co-ordinates of the locaton of the point source respectively.

For the numerical solution, the present computer code is used in a domain of size 18 units × 12 units × 12 units. Other inputs are $T_0 = 0$ unit, $P = 10$ units, $k = 1$ unit, $U = 10$ units, $\alpha = 1$ unit. The point source is located at $x_{point} = 6$ units, $y_{point} = 12$ units and $z_{point} = 0$ unit. Tempearture values obtained by the three-dimensional diffusion model on a line AB, which is located at $z = 0.04$ units, are compared with the analytical solution given above and a good match is found between them [35]. Also, the analytical temperature fields on the top plane EFGH and the symmetry plane CDEF are compared and both the predictions agree quite well.

2.3.3 Freezing of a gel

The following acceptance determines the precision of the created present numerical model by contrasting the forecasts and the distributed exploratory results. The present numerical code is accepted against the distributed consequence of Rewcastle et al.[18]. They considered a tissue-reproducing gel (1.4% gelatin arrangement) in a barrel shaped perspex geometry where they recorded the temperature of a solidifying gel by putting thermocouples at a separation of 10 mm from the axis of the probe. The phase change occurred in the temperature interim of $[-4^oC, 0^oC]$. Further, the blood stream and the

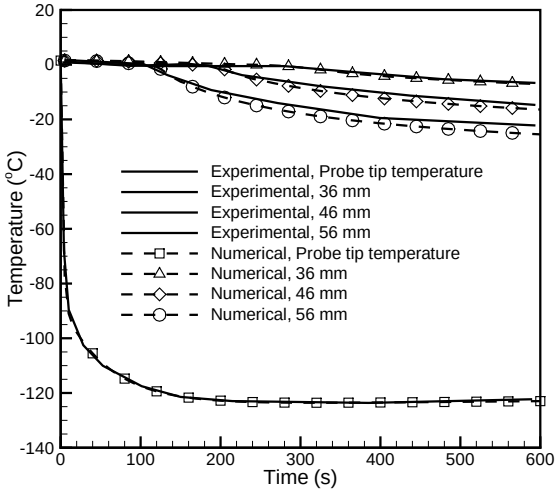

Figure 2.5: Temperature history at three locations

metabolic heat generations were not present for the gel. Figure 2.4 demonstrates a correlation between the processed temperatures, at the area of three thermocouples having organizes (10 mm, 36 mm), (10 mm, 46 mm), and (10 mm, 56 mm), and the trial temperatures acquired by Rewcastle et al. [18]. The exploratory slip on the temperature was assessed to $\pm 1.4^{o}C$ also, in this way, the present numerical results concur well with the distributed trial results.

CHAPTER 3

Results and Discussion

3.1 Generation of isotherm

The three dimensional numerical modelling is used to generate the isotherms within the ice ball. By taking the initial temperature of simulated ice ball to a uniform body temperature of 37^0C and modifying output enables the generation of isotherms about the cryoprobes at different times during the ice ball formation. Isotherms were generated for cryoprobe temperatures of -126^OC and -196^OC in a radial longitudinal plane for different configurations with and without central cryoprobe. Here isotherms were taken in sectional view and symmetrical view. It should be noted that because of symmetry of the problem results are obtained only for 1/8, 1/10 and 1/12 portion of the tissue and are presented in the following section.

Isotherms about the cryoprobe at 30, 60, 90, 150, 300 and 600s respectively from the flow of cryogen was initiated (10min) for different configurations. Isotherms for sectional view 30^0C , -0.53^0C , -40^0C , -75^0C , -110^0C and for symmetrical view 20^0C ,-0.53^OC , -20^0C -40^OC , -60^0C , -80^0C , -100^0C were plotted for the cryoprobe temperature of -126^OC (produced by the expansion of a high pressure gas usually argon or nitrogen), and -196^OC (produced by boiling of the liquid nitrogen) in the most appropriate plane of the iceball (20 mm from the cryoprobe tip).

Cancerous cell destruction occurs due to extra cellular ice formation between the temperature of -40^0C and -20^0C and intracellular ice formation temperature less than the -40^0C. However, lower end temperature -40^0C called lethal temperature, is considered for measuring of destruction of cancerous tissue. Temperature-0.53^0C considered as freezing temperature. The thermo physical properties of biological tissue are listed 3.1. The lethal front propagation for various configurations are obtained on ax-

ial plane which coincide with z-plane passing through middle of active length of cryoprobe (Z=50mm). Below description gives the comparative study on different parameters among different cryoprobe configurations.

3.2 Comparision of isotherm between configuration 1 and 2 for cryoprobe temperature at $-126^{O}C$

Figures3.1,3.3 with different timings reperesent for configuration 1 and 2. Due to the presence of central probe more heat exchange is available which results in frequent thermal interaction between the ice balls. this effect is noticed at 30s for configuration 1 as shown in 3.1. When it comes to configuration 2 only individual sub cooled ice ball can be observed without any thermal interaction and coalescence is noticed at 60s. Thermal interaction continued in either of configurations up to 150s. As the time goes on incresing distance between any two isotherms reduces and thermal conductivity increases then, the interaction of sub cooled ice balls occurs at lower temperature levels. It is also evedent from figure 3.1 that all the isotherms have remarkable changes in configuration 1. But, in the case of configuration 2 isotherm at $-110^{0}C$ has no any changes. finally it attains approxiamtely a spherical shape. At the end of freezing process lethal and freezing front travel 0.019m and 0.0255m respectively for configuration 1, when it comes to configuration 2, 0.0185m and 0.025m respectively. Isotherms of configuration 1 is more denser than the configuration 2 which causes effective necrosis of biological tissue. It is observed from the figures 3.1and 3.2.

3.3 Comparision of isotherm between configuration 1 and 2 for cryoprobe temperature at $-196^{O}C$

Figures 3.4,3.6 shows except at 30s lethal and freezing front propagation for configuration 1 and 2 at cryoprobe temperature $-196^{O}C$ are almost same for remaining timings. At 30s configuration 2 has no appreciable growth in lethal front. whereas, in configuration 1 lethal front moves very rapidly. As above said, thermal conductivity increases with increase in time by reducing the distance between any two isotherms and thermal interactions occur at lower level, in addition to this here cryoprobe temperature is also decreased. So that the changes occured in slope of isotherms can be observed at lower levels i.e at -$145^{0}C$ and $-180^{O}C$ for configuration 1. For configuration 2 change in slope of -$145^{0}C$ isotherm observed at 90, 150, 300, 600s. Due to decrease in cryoprobe temperature, Isotherm at $-180^{O}C$ in configuration 2 does not get the adequate amount of temperature gradient. Whereas, in configuration 1 presence of central probe causes active thermal interaction of all the isotherms. Even it is attained to spherical shape,

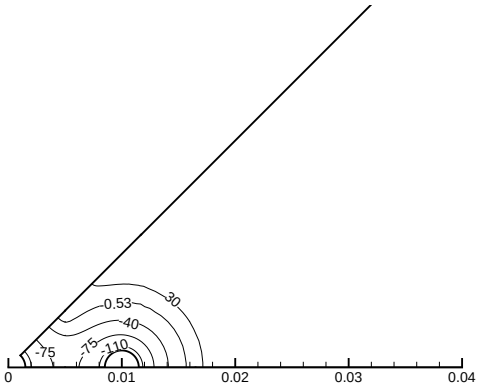

(a) 30s

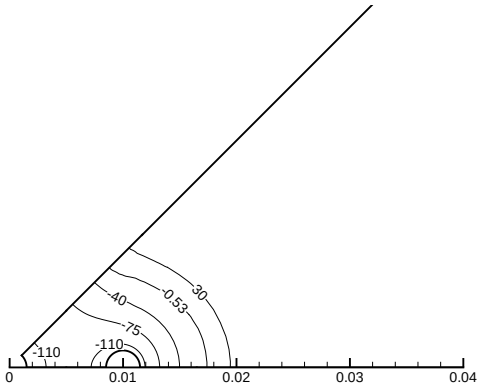

(b) 60s

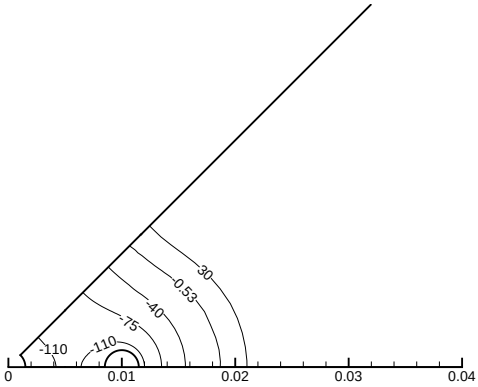

(c) 90s

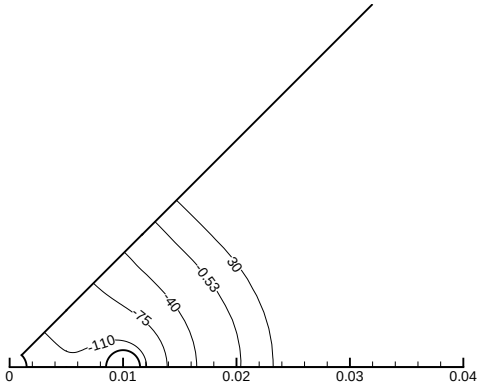

(d) 150s

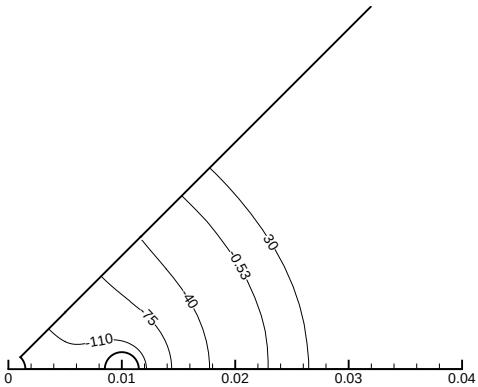

(e) 300s

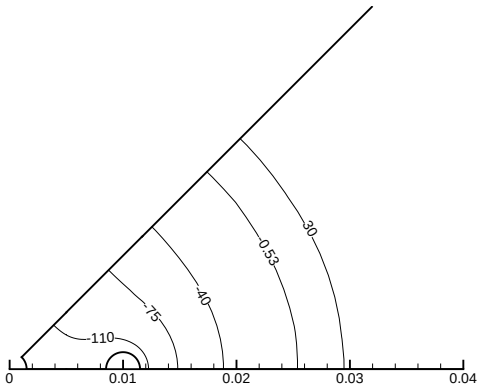

(f) 600s

Figure 3.1: Sectional view of isotherms for configuration 1 at -126 ^0C

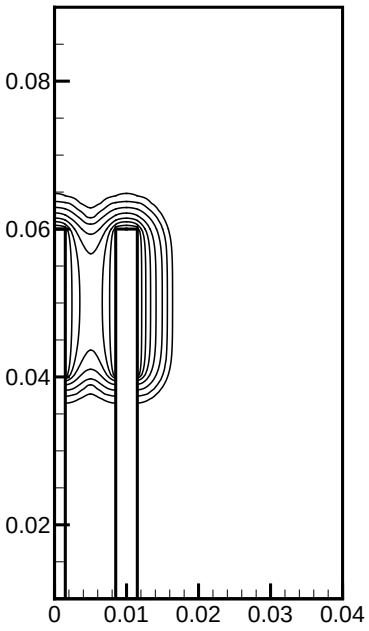

(a) 30s

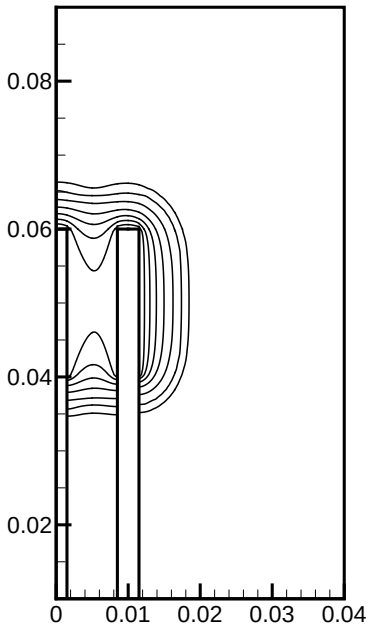

(b) 60s

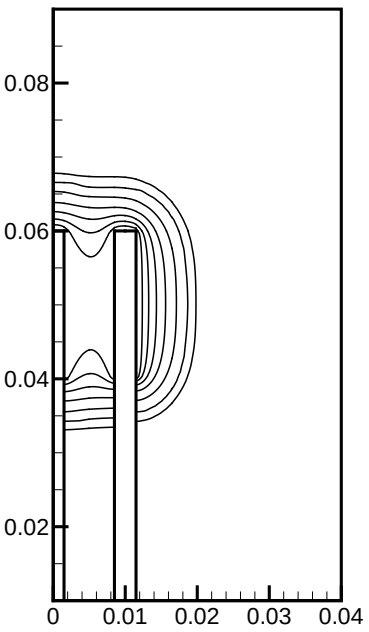

(c) 90s

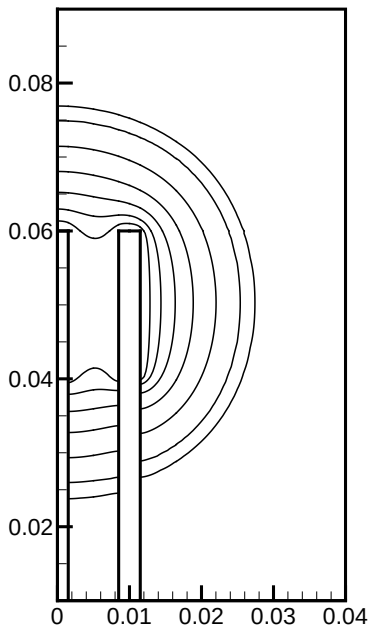

(d) 600s

Figure 3.2: Symmetrical view of isotherm for configuration 1 at $-126^{O}C$

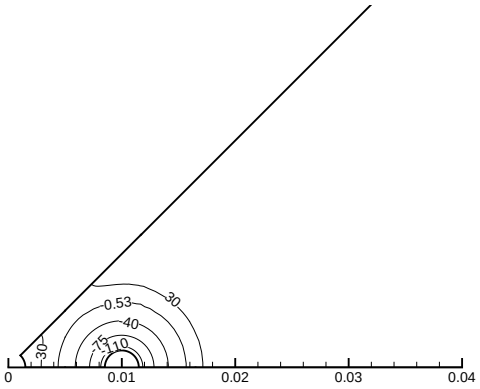

(a) 4t1-30sec

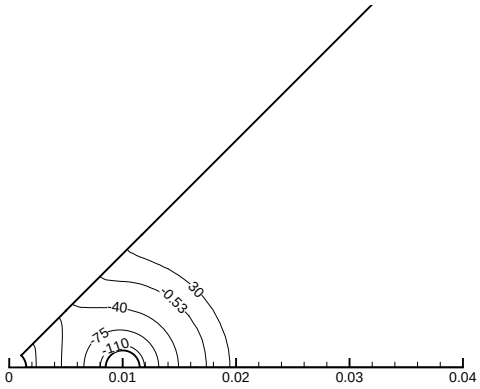

(b) 4-126-60sec

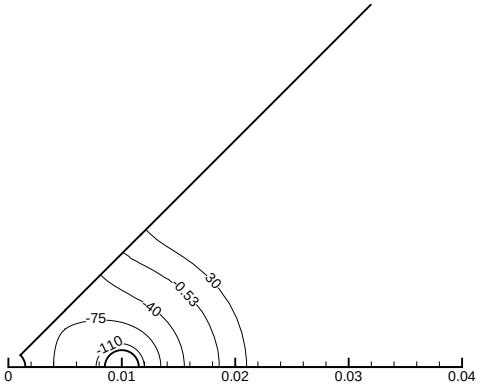

(c) 4-126-90sec

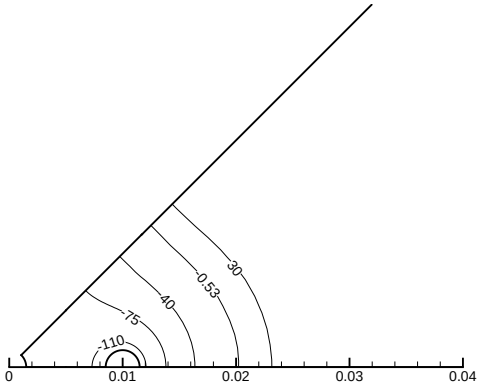

(d) 4-126-150sec

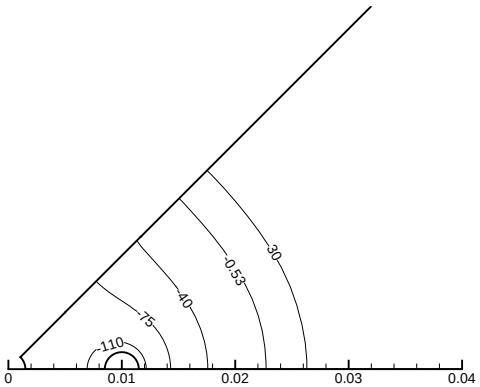

(e) 4-126-300sec

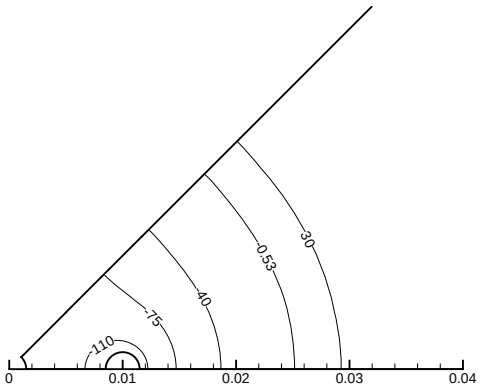

(f) 4-126-600sec

Figure 3.3: Sectional view of isotherms for configuration 2 at -126 ^0C

steady state is not achived in either of the cases. at the end of freezing process lethal and freezing front travel axially 0.024m and 0.034m for both configurations.

It is noticed that at the end of freezing process decrease in cryoprobe temperature results is increase in individual lethal and freezing front volumes for both the configurations, simultaneously the percentage of increase in lethal and freezing front volumes with central probe to without central probe is decreasing. It is also noticed that the lethal front propagation is higher in axial direction than the symmetrical direction.

3.4 Comparision of isotherm between configuration 5 and 6 for cryoprobe temperature at $-126^{O}C$

Figures 3.7,3.8 and 3.9 show the isotherm generation for configuration 5 and 6 for cryoprobe temperature $-126^{O}C$. Being central cryoprobe surrounded by six offset cryoprobes, at 30s: complete merging of ice ball can be observed for configuration 5. At the same time for configuration 6 partial merging i.e up to lethal temperature occured. The lethal and freezing front propagations in axial direction are same for configuration 5 and 6. Lethal and freezing isotherms are more spherical for configuration 5 than configuration 6. Due to presence of central probe, temperature gradient in configuration 5 is more than the configuration 6, so that in configuration 6 up to 90s there is no significant change in isotherm at -110^{o}C whereas in configuration 5 growth in isotherm at -110^{o}C taking place with respect to temperature. At the 90s iceball formed around the offset cryoprobes in configuration 6 reached to approximately spherical shape, but the distance between the center to center of ice balls surrounded by offset cryoprobes are not adequate to interact thermally. As the freezing time goes on increaseing, ice formation around the offset probe increases which results in decrease in central distance of the offset cryoprobes and increase in temperature gradient. At 150s the change in $-110^{o}C$ isotherm can be observed. Coming to the configuration 5 presence of central cryoprobe makes formation of ice centrally from the earlier timings.

3.5 Comparision of isotherm between configuration 5 and 6 for cryoprobe temperature at $-196^{O}C$

Figures 3.10,3.11 shows the generation of isotherms for configuration 5 and 6 at cryoprobe temperature $-196^{o}C$. Due to decrease in cryoprobe temperature from $-126^{O}C$ to $-196^{O}C$, At 30s configuration 5 has complete merging of all sub cooled iceballs formed around the offset cryoprobes with central probe, at the same time it is observed that evaluation of isotherms at the lower levels for configuration 6. The complete merging centrally for configuration 6 can be observed at 300s.

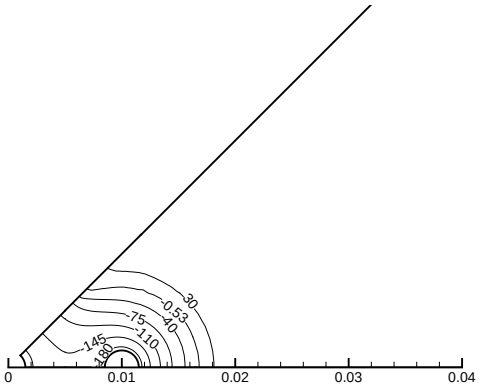

(a) 30s

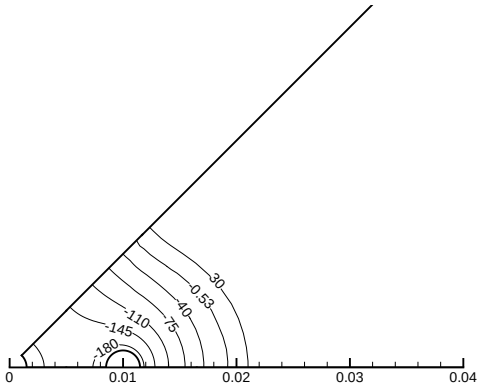

(b) 60s

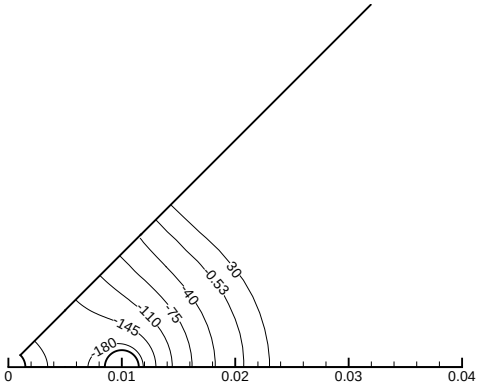

(c) 90s

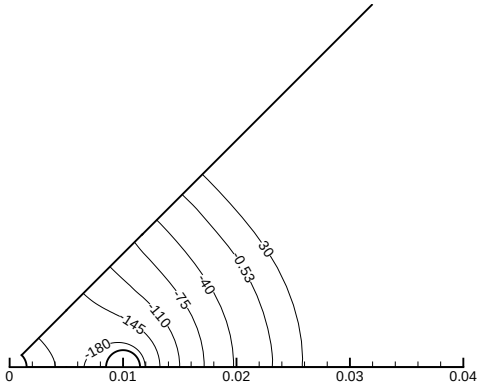

(d) 150s

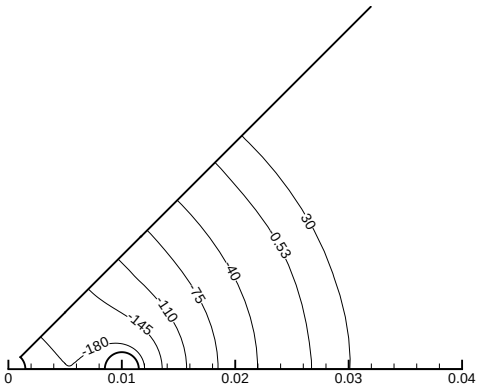

(e) 300s

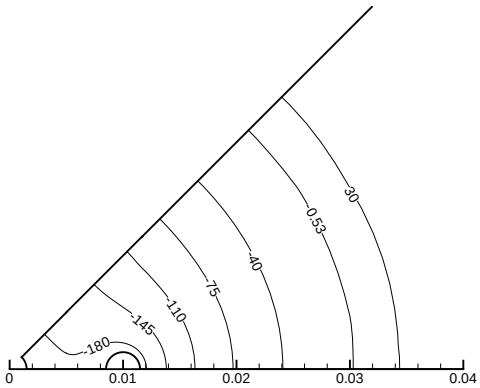

(f) 600s

Figure 3.4: Sectional view of isotherm for configuration 1 at $-196^{O}C$

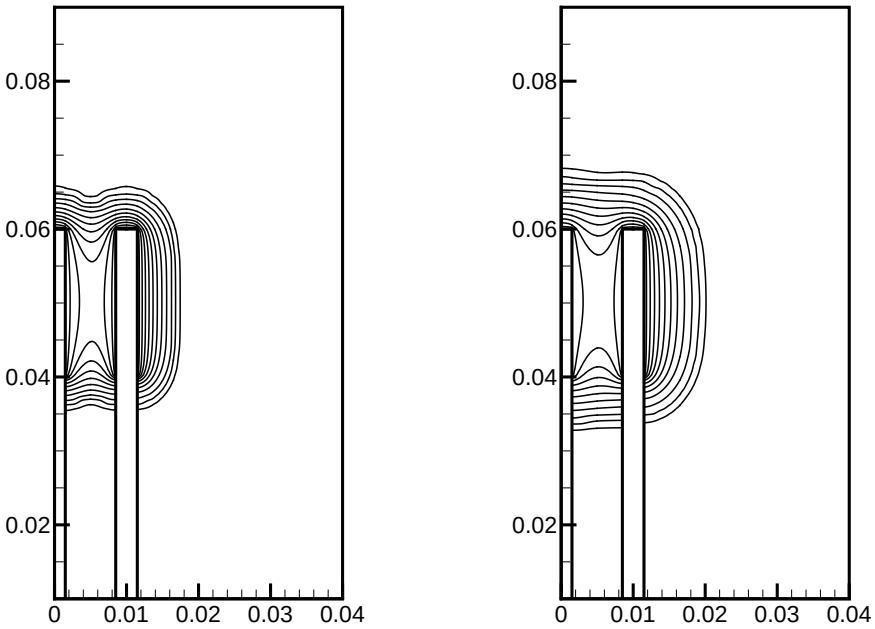

(a) 30s

(b) 60s

(c) 90s

(d) 600s

Figure 3.5: Symmetrical view of isotherms for configuration 1 at $-196^{O}C$

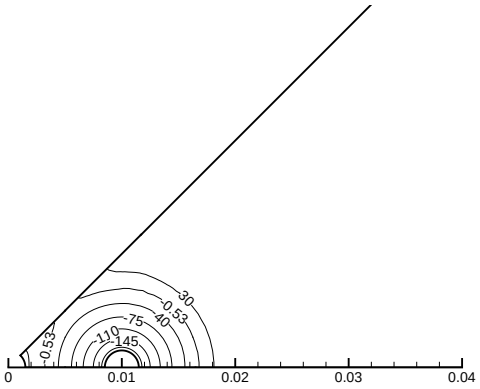

(a) 4-196-30sec

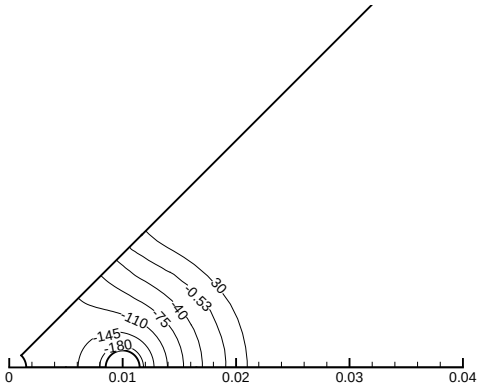

(b) 4-196-60sec

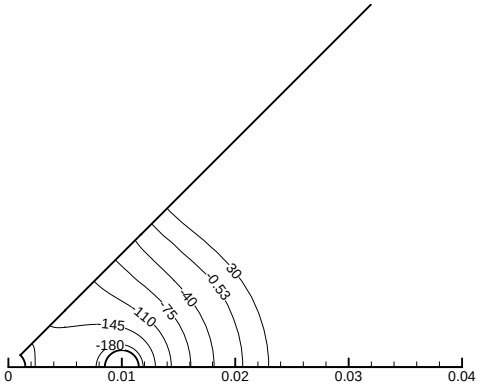

(c) 4-196-90sec

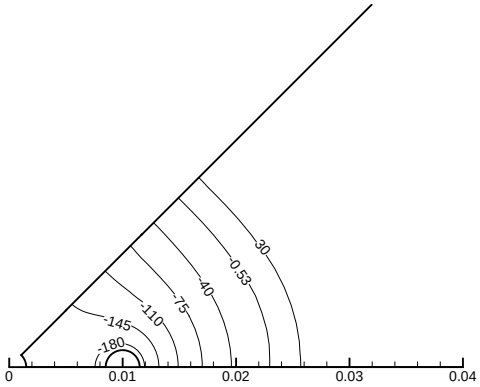

(d) 4-196-150sec

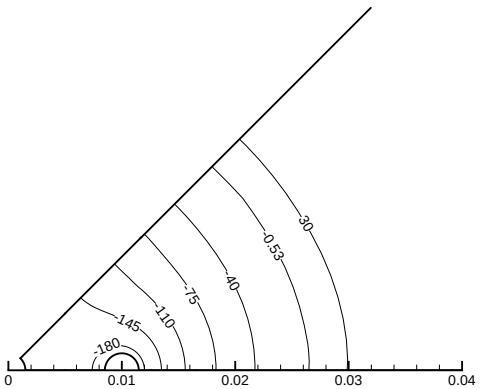

(e) 4-196-300sec

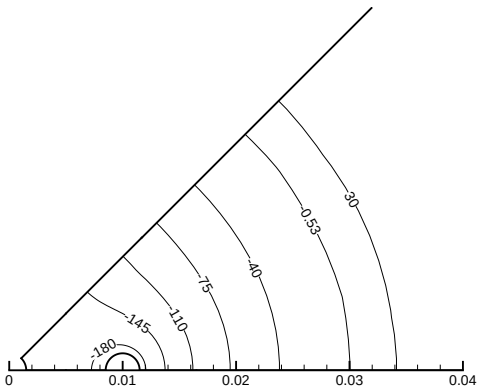

(f) 4-196-600sec

Figure 3.6: Sectional view of isotherm for configuration 2 at $-196^{O}C$

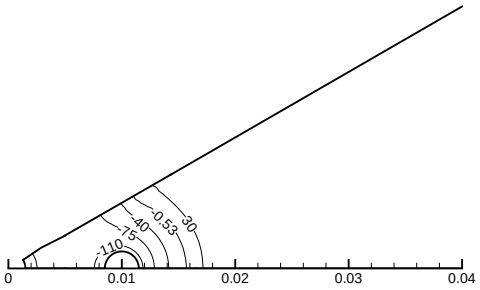

(a) 30s

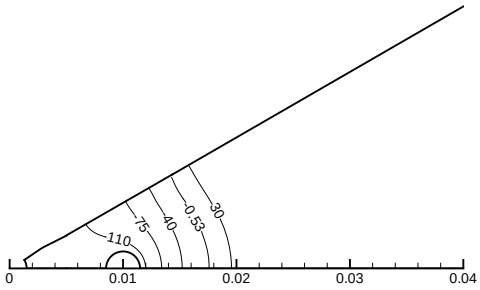

(b) 60s

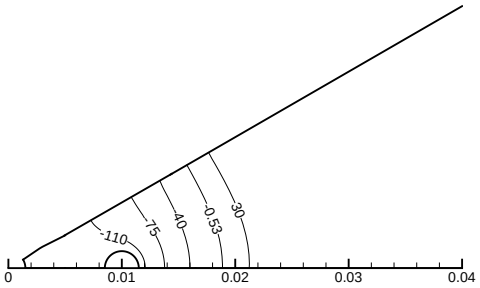

(c) 90s

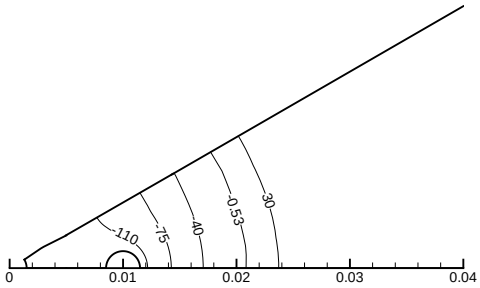

(d) 150s

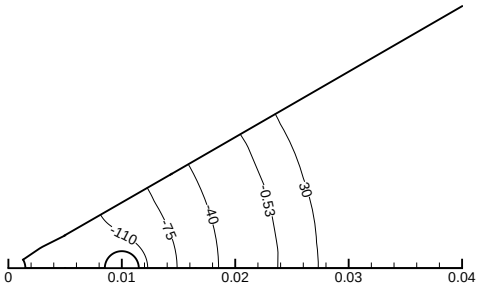

(e) 300s

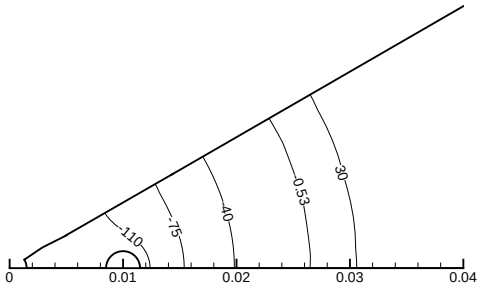

(f) 600s

Figure 3.7: Sectional view of isotherms for configuration 5 at $-126^{O}C$

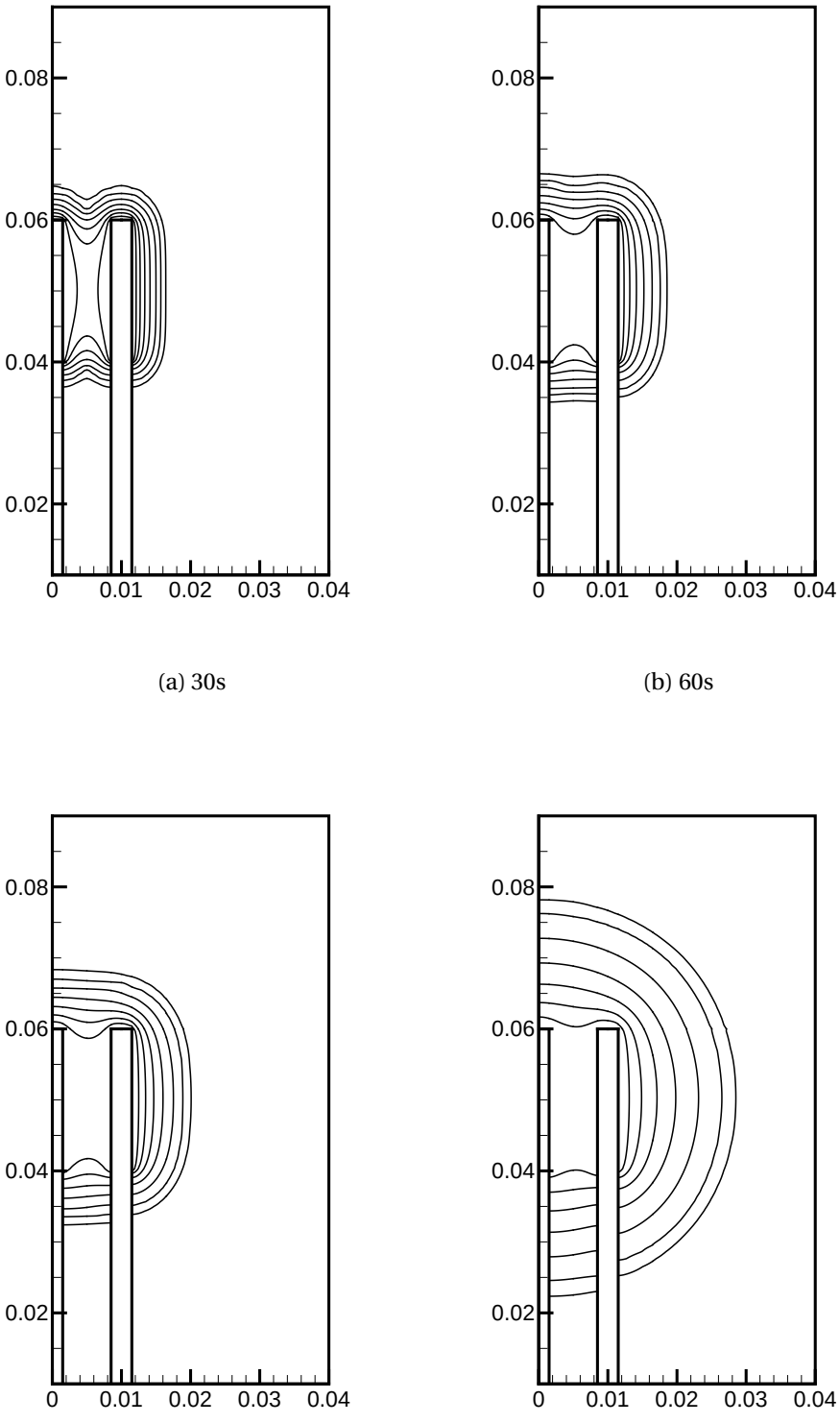

(a) 30s

(b) 60s

(c) 90s

(d) 600s

Figure 3.8: Symmetrical view of isotherms for configuration 5 at $-126^{O}C$

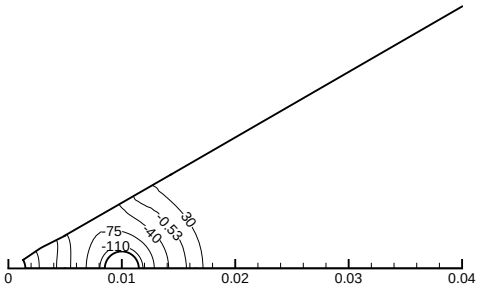

(a) 6-126-30sec

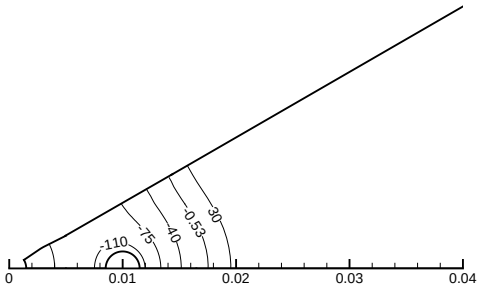

(b) 6-126-60sec

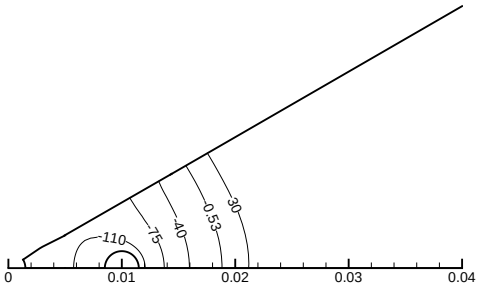

(c) 6-126-90sec

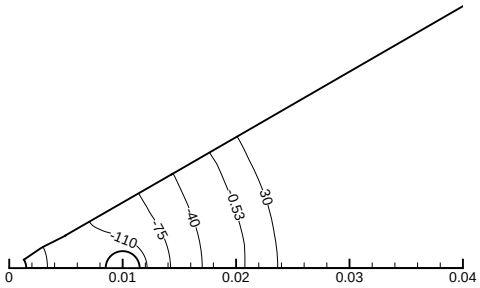

(d) 6-126-150sec

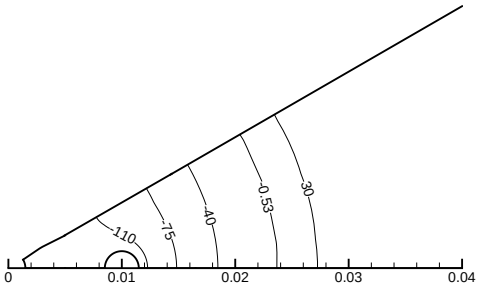

(e) 6-126-300sec

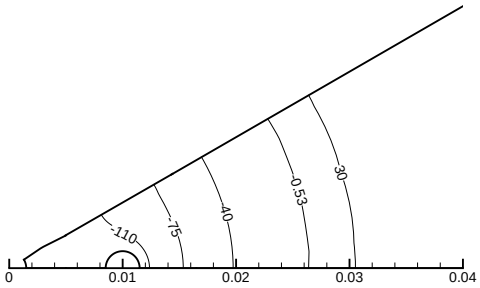

(f) 6-126-600sec

Figure 3.9: Sectional view of isotherms for configuration 6 at $-126^{O}C$

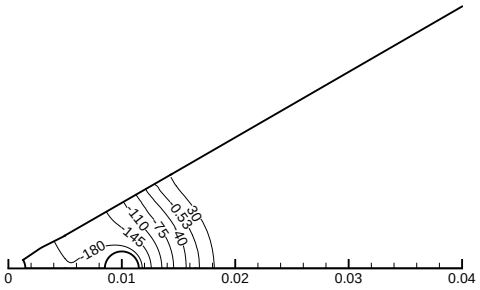

(a) 30s

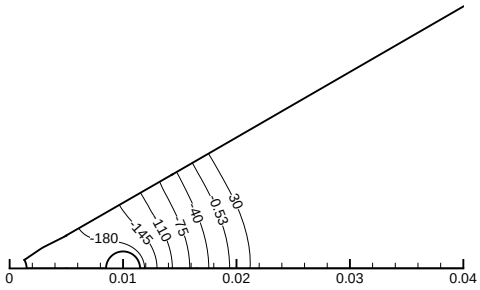

(b) 60s

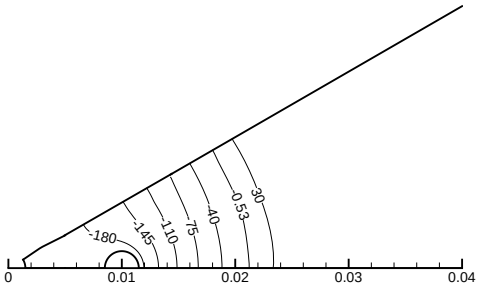

(c) 90s

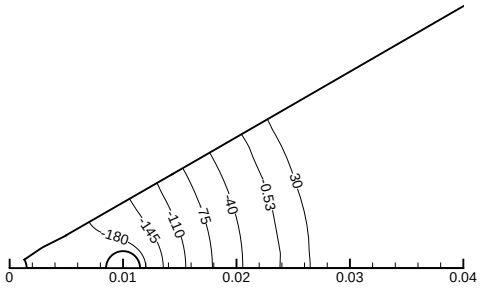

(d) 150s

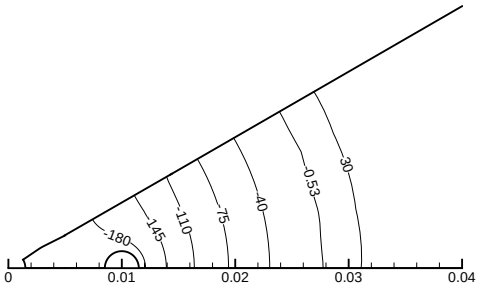

(e) 300s

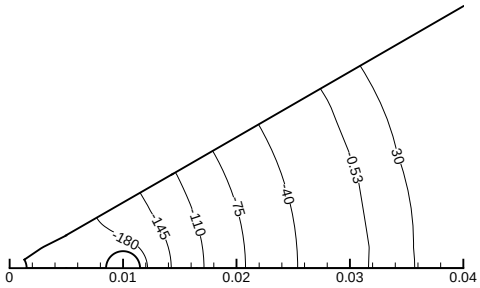

(f) 600s

Figure 3.10: Sectional view of isotherms for configuration 5 at $-196^{O}C$

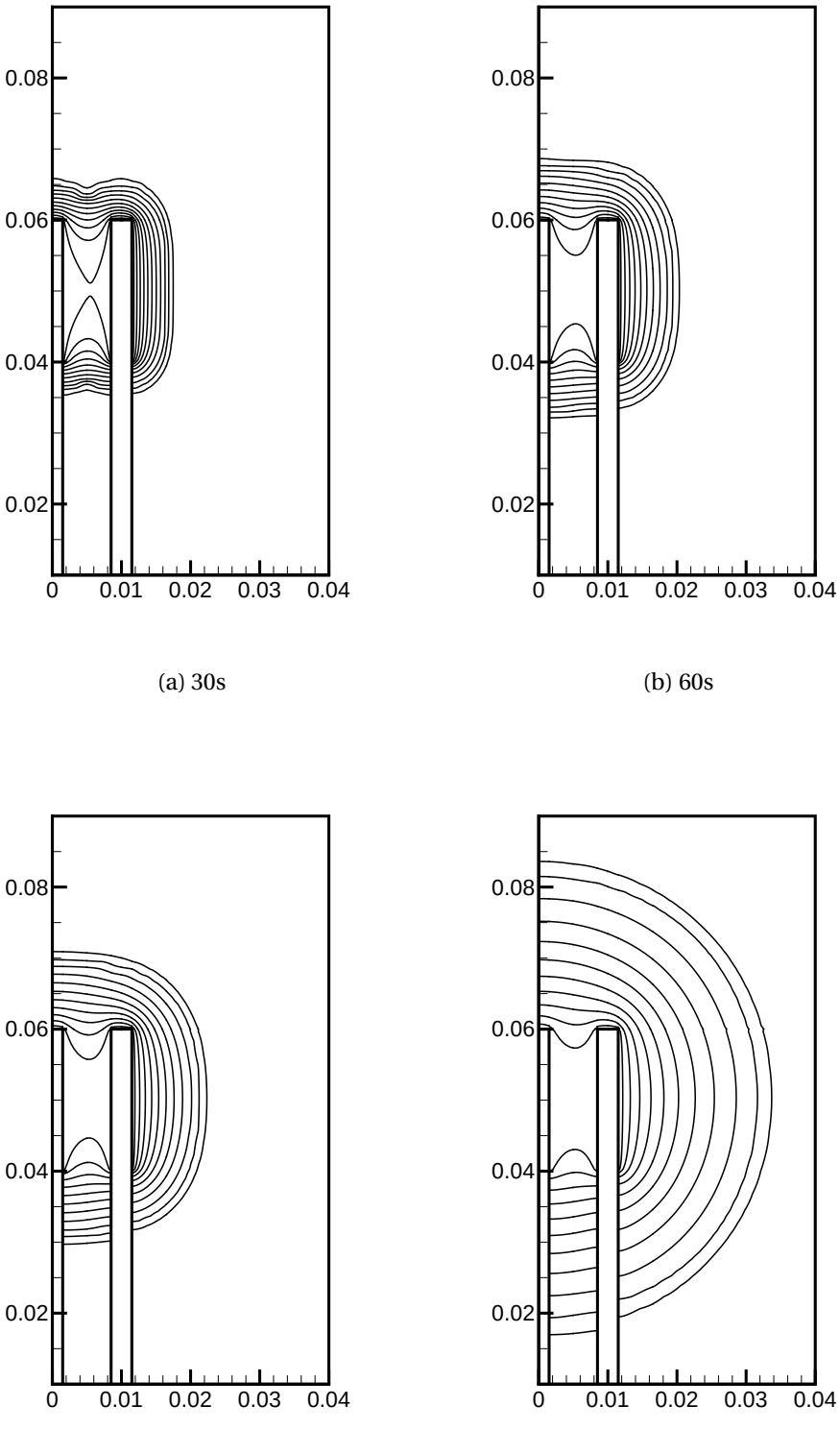

(a) 30s

(b) 60s

(c) 90s

(d) 600s

Figure 3.11: Symmetrical view of isotherms for configuration 5 at $-196^{O}C$

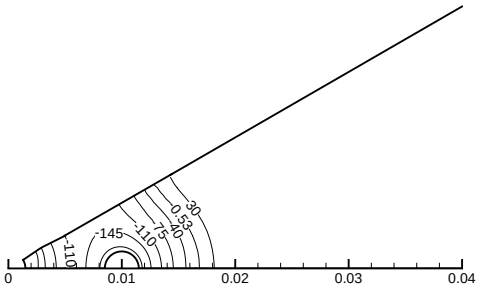

(a) 6-196-30sec

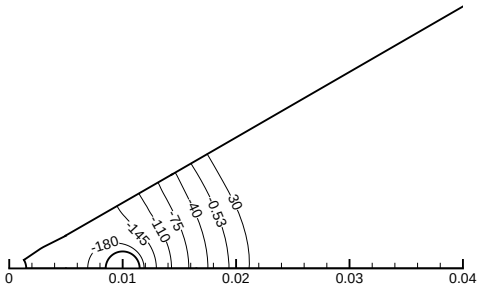

(b) 6-196-60sec

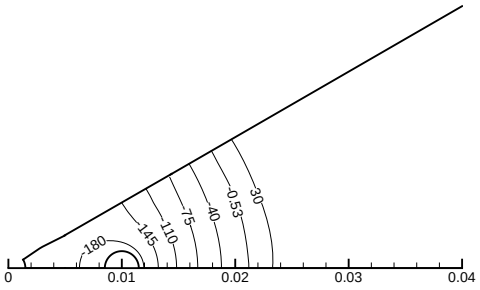

(c) 6-196-90sec

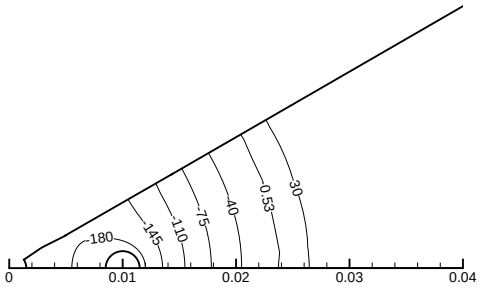

(d) 6-196-150sec

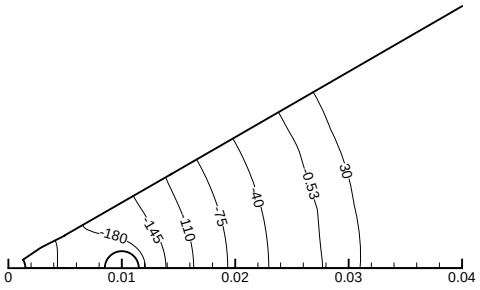

(e) 6-196-300sec

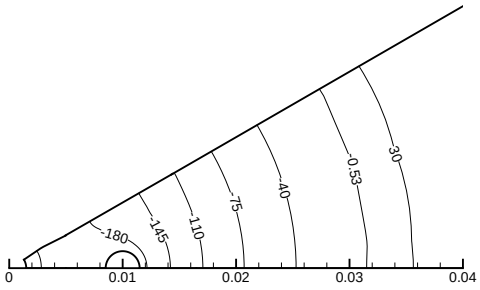

(f) 6-196-600sec

Figure 3.12: Sectional view of isotherms for configuration 6 at $-196^{O}C$

Table 3.1: Thermo -physical properties of biological tissue

ρ_u	999 kg/m^3	L	194×10^3 J/kg
ρ_f	921 kg/m^3	c_b	4200 J/kg^{o}C
c_{pu}	3230 J/kg^{o}C	k_u	0.325 W/m^{o}C
c_{pf}	$140 + 4.654(T + 273)$ J/kg^{o}C	k_f	$1.46 + 0.0038(-T)^{1.156}$ W/m^{o}C
T_l	-0.53°C	T_s	-8°C

3.6 Lethal front propagation

Cancerous cell destruction occurs due to extra cellular ice formation between the temperature of -4^0C and -21^0C and intracellular ice formation temperature less than -40^OC. However lower end temperature -40^OC called lethal temperature, is considered for measuring of destruction of cancerous tissue. The thermo-physical properties of a biological tissue are listed in Table3.1 . The lethal front propagation for various configurations are obtained on axial plane which coincide with the z-plane passing through the middle of the active length of the cryoprobe (z=50mm). It is evident from the figures 3.1,3.4,3.7,3.12 that the lethal front propagation along the axial plane increases very rapidly and reaches to steady state at the end of freezing process. Figures 3.2,3.5,3.8,3.11 depict that the propagation along the symmetrical direction differ from axial direction. Propagation in symmetrical direction follows three phases. In first phase the propagation of lethal front follows the same trend as that of axial plane because there is no thermal interaction between the individual sub cooled iceballs formed around the central and offset cryoprobes. Second phase starts at 24s and 18s for configuration 1 with cryoprobe temperature -126^OC and -196^OC respectively, and there is a sudden change in shape of the isotherms slope due to coalescence of individual sub cooled ice balls, and this process is very rapid in the symmetrical direction while it is 24 s and 16 s for configuration 5 at -126^OC and -196^OC respectively. Then, the third phase: sub cooled ice ball formed around the offset and central cryoprobe unite together at 250s and 150s for -126^OC and -196^OC temperatures, and attains steady state size slowly.

From the figures 3.1,3.4 the lethal front propagation for configuration 1 axial plane (along OA) at the end of freezing process of cryoprobe temperatures -126^OC and -196^OC are approximately 0.018m and 0.024m. Similarly it is 0.02m and 0.025m for configuration 5 from figures 3.7,3.10 . Figure3.13 depicts the lethal front propagation for the configuration 1&5. figures 3.13a,3.13b show that lethal front propagation for cryoprobe temperature -196^OC is always ahead to cryoprobe temperature -126^OC throughout the freezing process, and the difference between these two increase with respect to time. It is also evedent from the Table 3.2,3.3 . For the given freeze cycle of 10 min, the united sub-cooled ice ball did not attain the spherical shape for the configuration 1 irrespective of the cryoprobe temperatures. However, the sperical shape is attained for the configuration 5 at around 250 s and 150 s with cryoprobe temperature of -126^oC and -196^oC

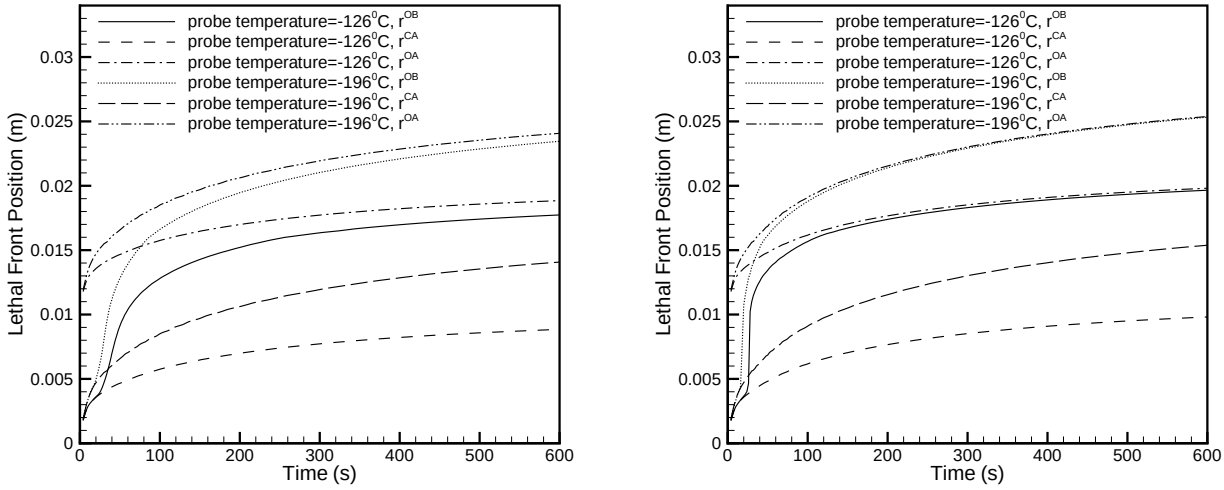

(a) Configuration 1

(b) Configuration 5

Figure 3.13: Lethal front propagation with time; r^{OB} is distance from O along line OB , r^{CA} is distance from C along line OA, and r^{OA} is distance from O along line OA (see figure1)

respectively. Though the united sub-cooled ice ball attained the spherical shape but it has not reached the steady state for any of the cases during the freezing cycle of 10 min.

3.7 Freezing and lethal ice ball volumes

Figure 3.14 shows that the volume enclosed by freezing front -0.53^OC and lethal front -40^OC for the cryoprobe temperature at -126^OC and -196^oC for different configurations. Left hand side figures indicate the -126^OC and right hand side figures indicate the -196^OC while top side figures indicate the frozen front volume, bottom side figures indicate the lethal zone volumes. From the isotherm figures it is evident that the volume enclosed by the frozen front isotherm -0.53^OC is tedious for all configurations. Figures 3.1,3.4,3.7,3.10 depict at 30 seconds the volume enclosed by lethal front isotherm first increases slowly and then there is change in volume, where the merging of two sub cooled ice balls formed around the offset and central cryoprobe along the symmetry plane r^{OB} (see figure 1). This phenomenon is more pronounced at -126^OC for all configurations . Figure3.14 shows that the volume of ice ball with central cryoprobe is always ahead compared to the corresponding configuration without ice ball throughout the freezing process. figures 3.1,3.4,3.7,3.10 depict that the difference in ice ball volume increases with increase in freezing time. Tables 3.2,3.3 shows the percentage of increase in ice ball volume for frozen(-0.53^OC) and lethal(-40^OC)zones at the end of freezing process (10min) for different configuration at -126^OC and -196^OC respectively.

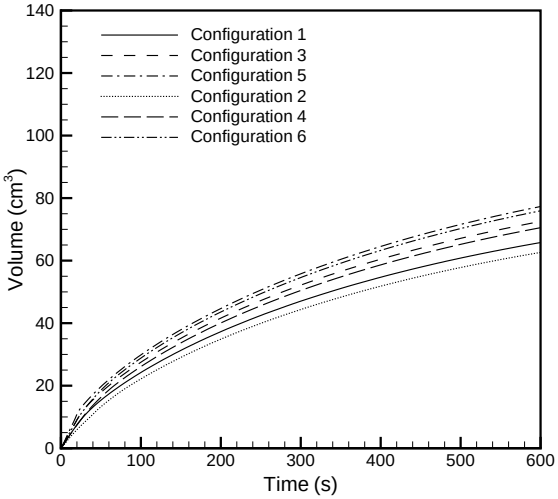

(a) -0.53^oC iceball, cryoprobe temperature = -126^oC

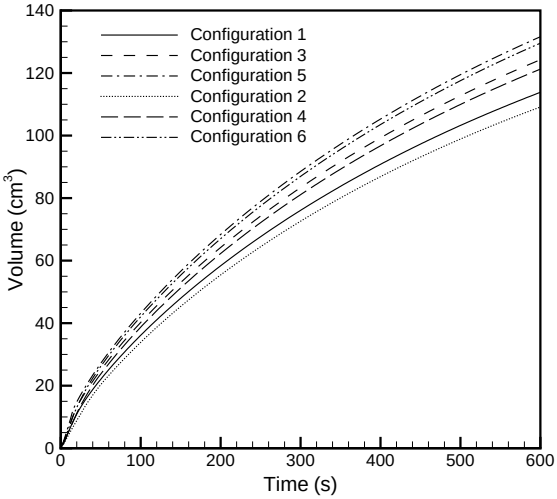

(b) -0.53^oC iceball, cryoprobe temperature = -196^oC

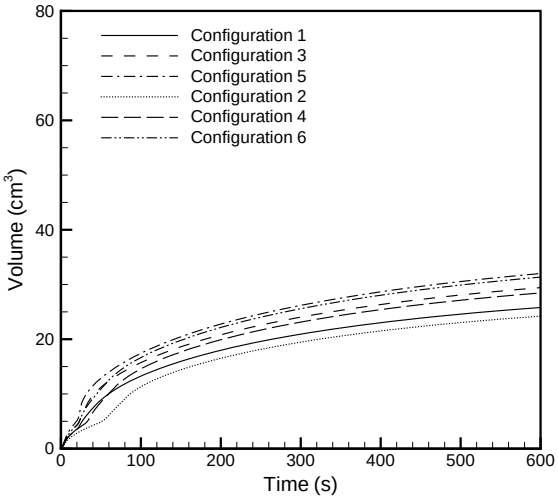

(c) -40^oC iceball, cryoprobe temperature = -126^oC

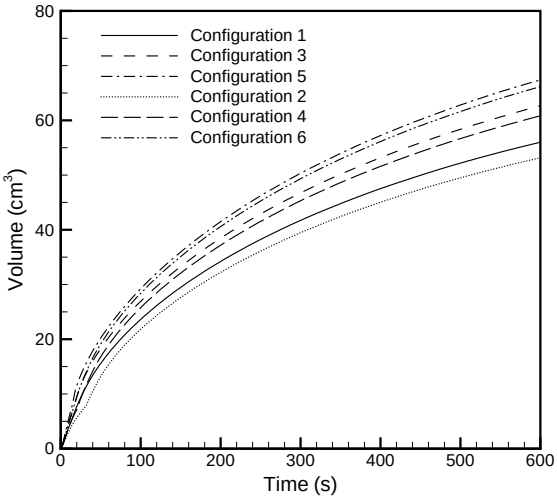

(d) -40^oC iceball, cryoprobe temperature = -196^oC

Figure 3.14: Variation of frozen volume for different configurations

Table 3.2: Percentage of increase in ice ball volume for frozen($-0.53^{O}C$) and lethal($-40^{O}C$)at the ed of freezing process (10min) for different configuration for cryoprobe temperatures $-126^{O}C$

Configuration	Volume of the ice ball with central probe	Volume of the ice ball without central probe	% of increase in iceball volume	Cryoprobe temperature T_P
1	65.77	62.62	5.03	$-0.53^{O}C$
3	72.535	70.539	2.82	$-0.53^{O}C$
5	77.310	75.932	1.81	$-0.53^{O}C$
1	25.793	24.209	6.54	$-40^{O}C$
3	29.433	28.455	3.43	$-40^{O}C$
5	32.007	31.350	2.09	$-40^{O}C$

Table 3.3: Percentage of increase in ice ball volume for frozen($-0.53^{O}C$) and lethal($-40^{O}C$)at the ed of freezing process (10min) for different configuration for cryoprobe temperatures $-196^{O}C$

Configuration	Volume of the ice ball with central probe	Volume of the ice ball without central probe	% of increase in iceball volume	cryoprobe temperature T_P
1	113.83	109.10	4.335	$-0.53^{O}C$
3	124.24	121.23	2.48	$-0.53^{O}C$
5	131.59	129.54	1.582	$-0.53^{O}C$
1	55.999	53.167	5.32	$-40^{O}C$
3	62.678	60.835	3.02	$-40^{O}C$
5	67.397	66.168	1.85	$-40^{O}C$

The percentage increase in ice ball volume (obtained at the end of freezing cycle, i.e. 10 min considering with and without central cryoprobe configurations) decreases with increase in number of offset cryoprobe if they are kept at same temperature.

The effect of cryoprobe temperature T_p on the percentage change in ice ball volumes (both the frozen zone and the lethal zone) is presented in Table 3.4. It should be noted that these values are obtained at the end of freezing cycle, i.e. after 10 min of freezing operation. It is interesting to observe from the Table 3.4 that the percentage increase in volume remains less than 75% for frozen ice ball volume, it is more than 110% for lethal ice ball volume showing the strong dependence of tissue necrosis on the cryoprobe operating temperature. Also, the increase in number of offset cryoprobe have insignificant effect on the percentage increase in ice ball volumes.

Table 3.4: Percentage increase in iceball volume, V_i, with cryoprobe temperature, T_P

Configuration	% increase in V_i with a central cryoprobe, when T_P changes from -126^oC to -196^oC	% increase in V_i without a central cryoprobe, when T_P changes from -126^oC to -196^oC	Frozen and lethal front temperatures
1	73.05	74.21	-0.53^oC
3	71.29	71.87	-0.53^oC
5	70.21	70.60	-0.53^oC
1	117.18	119.58	-40^oC
3	112.98	113.81	-40^oC
5	110.53	111.07	-40^oC

Figure3.15 shows the formation of iceball for frozen (-0.53^OC) and lethal zones (-40^OC) for configuration 1 and 5. For comparision purpose volume obtained for the far apart cryoprobe was also plotted. The figure 3.15 (a), (b),(c),(d) shows that –0.53^0C iceball volume obtained by the far apart placed cryoprobes is always more than the volume obtained by any other configurations,But it is reverse at -40^oC for cryoprobe temperature -126^OC, being central probe surrounded by offset probes evalution of iceball formed around the central probe resticted by offset cryoporbes which results in high temperature gradient at the central cryoprbe and more heat transfer takes place. The difference in volume between the studied configurations and far apart cryoprobe is increases with decrease in cryoprobe temperature and increase in number of offset cryoprobes. In studied configurations as the cryoprobe temperature decreasing from -126^oC to -196^oC temperature gradient lower than the far apart cryoprobe, which results in volume enclosed by far apart cryoprobes higher than respective configurations. From the figures 3.15 (b),(d) it is observed that with decrease in cryoprobe temperature from -126^OC to -196^OC volume enclosed by the -40^oC far apart placed cryoprobes is greater than the corresponding configurations.

3.8 Ablation ratio

It is defined as the ratio of volume enclosed by ablative temperature, specific to tissues –40^0C to the total frozen ice ball volume (–0.53^0C for this study). Figure3.16 depicts the ablation ratio for different configurations for both the operating temperatures of cryoprobes, i.e. –126^0C and –196^0C . For comparative study, the ablation ratio of the far apart placed cryoprobes is also presented.

Ablation ratio for far apart placed cryoprobe decreases monotonically and reaches to steady state because of the blood perfusion and surrounding blood acting as a sink.

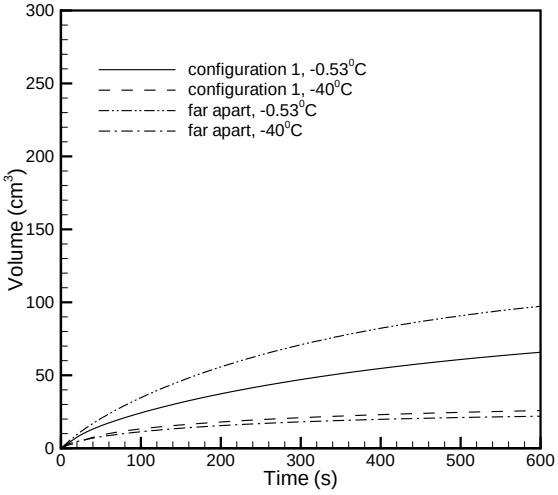

(a) Cryoprobe temperature $T_p = -126^o C$

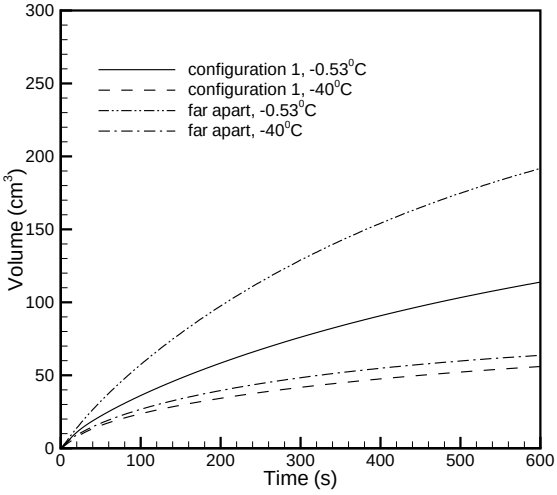

(b) Cryoprobe temperature $T_p = -196^o C$

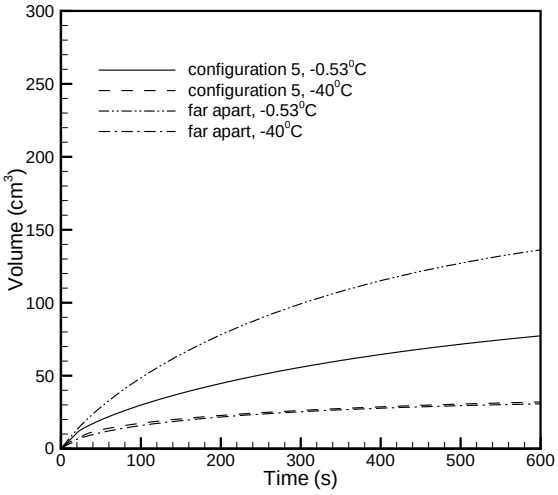

(c) Cryoprobe temperature $T_p = -126^o C$

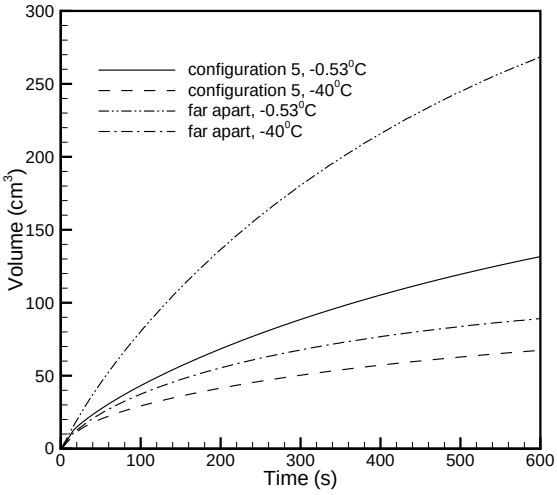

(d) Cryoprobe temperature $T_p = -196^o C$

Figure 3.15: Comparision of frozen volume variation

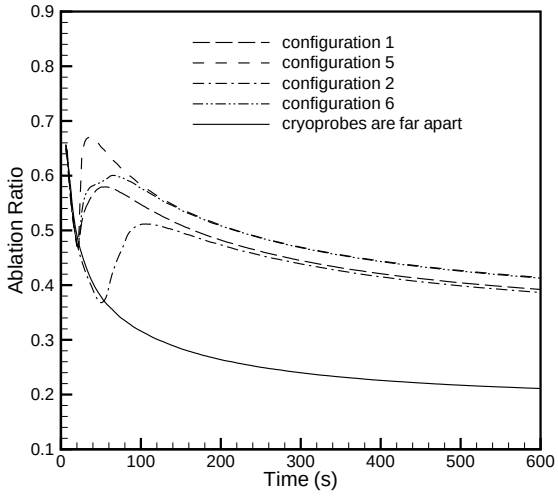

(a) Cryoprobe temperature of $-126^{o}C$

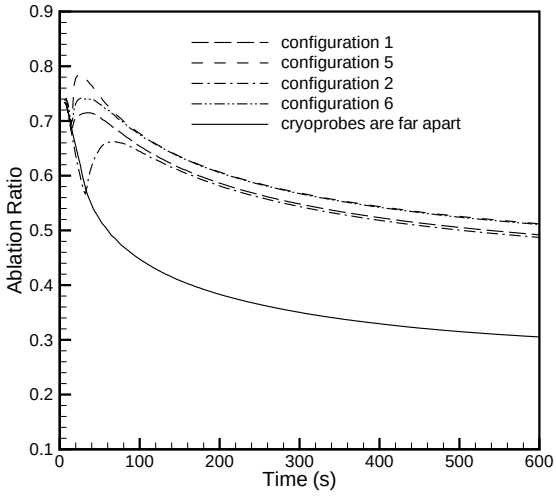

(b) Cryoprobe temperature of $-196^{o}C$

Figure 3.16: Ratio of volume enclosed by $-40^{o}C$ ice ball to the total frozen volume for different configurations

Table 3.5: Ablation ratio for different cryoprobe configuration after the 10min freezing cycle

Configuration	With central probe	without central probe	% of increase in ablation ratio	cryoprobe temperature ($T_P{}^0c$)
1	0.392	0.386	1.55	$-126^{O}C$
3	0.405	0.403	0.49	-126°C
5	0.414	0.412	0.2	-126°C
1	0.491	0.487	0.008	-196°C
3	0.504	0.501	0.005	-196°C
5	0.512	0.510	0.003	-196°C

Initially ablation ratio for different configuration is same as that of far apart cryoprobe. Later on, there is a drastic increase in ablation ratio, after that steady state is attained. These occurrences are due to colliding of any of the two ice ball surrounded by cryoprobe during the freezing process and becoming in to single spherical ice ball. From the table3.5 it can be observed that the effect of cryoprobe temperature and number of offset cryoprobes not noteworthy at the ending of freezing process. Ablation ratio for different configurations are given in below table for different cryoprobe temperatures after 10min freezing cycle. From the figure3.16 and table3.5 It is interesting to observe that irrespective of the number of cryoprobes and the operating temperature of cryoprobes, central cryoprobe has not that much effect on the ablation ratio at the end of freezing cycle. However, the effect of central cryoprobe can be noticed for freezing duration between 0min to 3min of the freezing cycle. Also, the effect is more remarkable

Table 3.6: Percentage of change in ablation ratio at which maximum difference occurred time.

Configuration	With central probe	Without central probe	Maximum Percentage of increase in ablation ratio	Time at which maximum % of increase in ablation ratio	Cryoprobe Temperature
1	0.5791	0.368	57.00%	52 s	$-126^{O}C$
3	0.6312	0.510	23.76%	46 s	-126°C
5	0.670	0.578	16.00%	36 s	-126°C
1	0.714	0.566	26.00%	32 s	-196°C
3	0.754	0.687	09.75%	30 s	-196°C
5	0.785	0.741	06.00%	26 s	-196°C

for the case with less number of offset croprobes and with lower operating temperature of cryoprobe. Table3.6 gives the maximum percentage of increase in ablation ratio for different configuration and their corresponding timings for respective temperatures. From the table3.6 it is observed that as the number of offset cryoprobes increases the maximum percentage of increase in ablation ratio with central probe to without central probe goes on decreasing, vice-versa, And it is also reduced with decrease in cryoprobe temperature.

3.9 Cooling power requirement

Figure3.17 shows the cooling power requirement for the different configuration of cryoprobe temperatures and also cooling power requirement for far apart cryoprobes during freezing process. Cooling power for the cryoprobe can be calculated by using given formula:

Cooling power = $k * A * \frac{dt}{dx}$

Where

1. K is thermal conductivity of frozen region adjacent to cryoprobe surface
2. A is the surface area of the active part of cryoprobe
3. dt/dx is the temperature gradient adjacent to active cryoprobe surface

From the figure 3.17 Initially the cooling power required by the far apart cryoprobe is more but as the time goes on increasing cooling power required by the far apart cryoprobe attains steady state with respect to time in entire freezing process. The reason is that during the starting of freezing process temperature gradient near the active surface of cryoprobe is high, in that period cooling power will be in peaks. With precedence

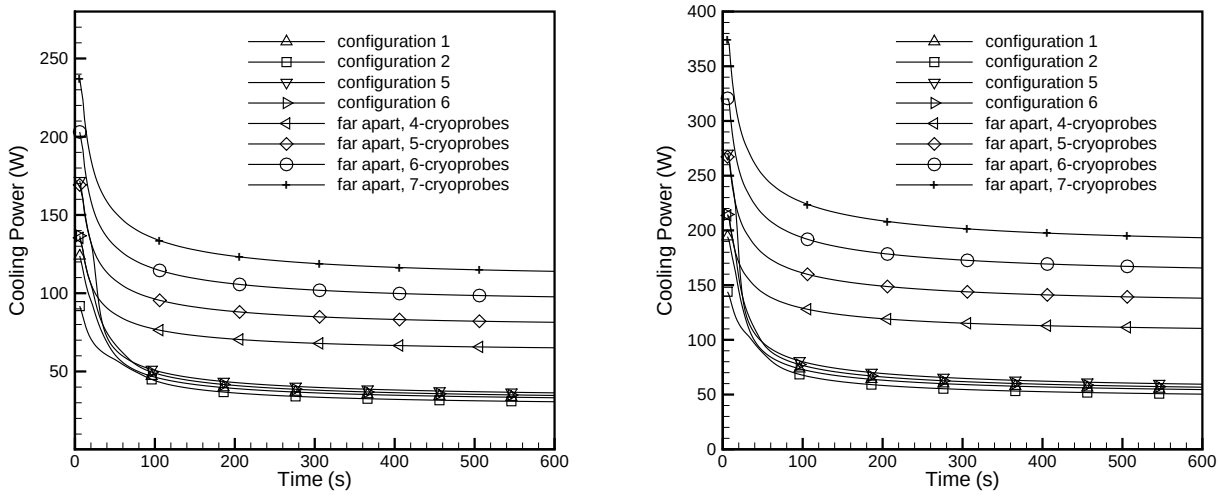

(a) Cryoprobe temperature of -126^oC

(b) Cryoprobe temperature of -196^oC

Figure 3.17: Cooling power absorbed by the cryoprobes

Table 3.7: Cooling power(in Watts) required by the different configurations at the end of freezing process (10min)

Configuration	With central probe	Without central probe	% of increase in cooling power	Cryoprobe temperature T_P
1	33.21	30.66	8.31	-126°C
3	35.17	33.14	6.12	-126°C
5	36.33	34.66	4.81	-126°C
1	54.54	50.37	8.27	-196°C
3	57.64	54.33	6.09	-196°C
5	59.46	56.73	4.81	-196°C

of time there was formation of ice around the cryoprobe. Hence temperature gradient at the surface of the cryoprobe is being reduced. During this period the cooling power required by the cryoprobe attains steady state. Being central and offset cryoprobes together with prescribed equal distance in the studied configurations, the temperature gradient is less between the central and offset cryoprobes, which results in less cooling power requirement than the far apart respective number of cryoprobes from starting onwards. Cooling power required by the different configuration are given in below table From the Table3.7 it can be observed that cooling power requirement increases with increase in number of offset cryoprobes and also increases with decrease in cryoprobe temperature keeping the other parameters same during the freezing process. It is also interesting to observe that, as the number of offset cryoprobes increases, the percentage of increase in cooling power with central probe to without central probe decreases. This

Table 3.8: Cooling power(w) requirement and pecentage of increase in cooling power at which the time, the maximum increase in percentage of ablation ratio obtained for different configurations.

Confi-guration	Time	Ablation ratio with central probe	Ablation ratio with-out central probe	Maximum % of in-crease in ab-lation ratio	Cryoprobe temperature T_P	Cooling power with central probe	Cooling power with-out central probe	% of increase in cooling power
1	52 s	0.5791	0.368	57	$-126^{O}C$	59.58	57.01	4.5
3	46 s	0.6312	0.510	23.76	$-126^{O}C$	66.36	67.13	1.16
5	36 s	0.670	0.578	16	$-126^{O}C$	77.57	78.70	1.45
1	32 s	0.714	0.566	26	-196°C	111.5	103.6	7.5
3	30 s	0.754	0.687	09	-196°C	121.3	121.3	0.032
5	26 s	0.785	0.741	06	-196°C	133.4	135.9	1.85

shows the insignificant effect of central cryoprobe on higher cryoprobe configurations. The below table depicts that the cooling power requirement and pecentage of increase in cooling power at which the time, the maximum increase in percentage of ablation ratio obtained for different configurations.

For increase in 4.5% of cooling power withcentral cryoprobe to without central cryoprobe for configuration 1 at 52 sec, the ablation ratio increased to 57% whereas it is 1.45% for configuration 5 at 36sec, ablation ratio increased to 16% keeping the both configuration at -126^{o}C. For decrease in cryoprobe temperature to –196^{0}C, increase in cooling power 7.5% and 1.85%, maximum pecentage of increase in ablation ratio 26% and 6% for configuration 1 and 5 respectively. From this important note, it is observed that the tissue necrosis can be done effectively with the effect of central cryoprobe at lower cryoprobe operating temperatures.

Contribution to cooling power by central and offset probes can be defined as the ratio of coling power of central cryoprobe to the cooling power absorbed by central and offset probe or cooling power of offset cryoprobe to the cooling power absorbed by central and offset cryoprobe. Figure shows 3.18 the contribution of cooling power for central and offset cryoprobe with respect to time. The scope of this observation is to find whethere the two cryoprobes are contributing to cooling power equally or not. It is interesting to observe that the percentage of contribution to cooling power by either of the cryoprobes independent of cryoprobe operating temperature. Due to symmetry of the problem only one offset cryoprobe was considered to calculate the percentage of contribution to cooling power. The contribution to cooling power for central probe initially is

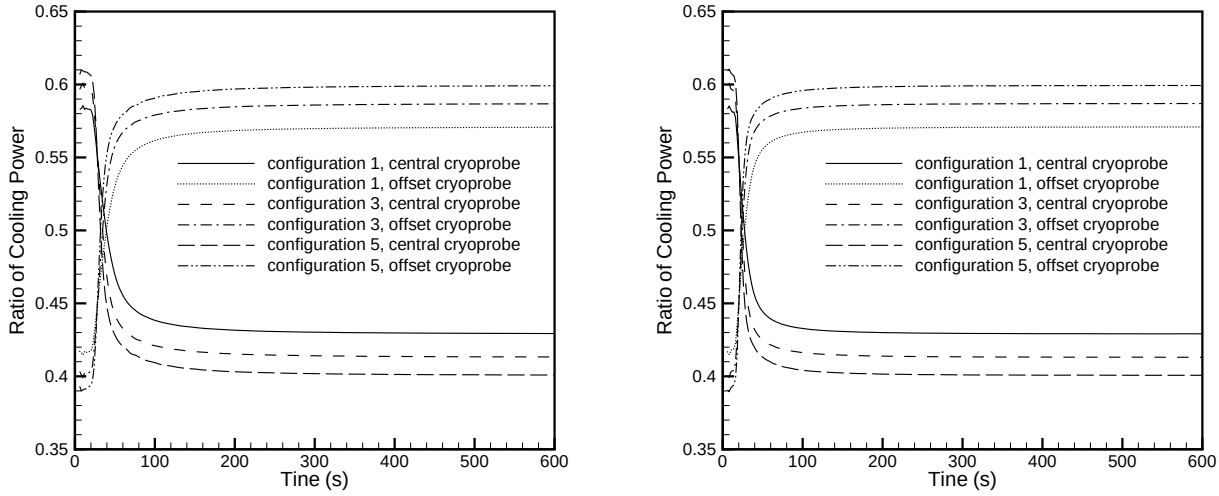

(a) For cryoprobe temperature -126^oC

(b) For cryoprobe temperature -196^oC

Figure 3.18: Contribution of absorbed cooling power by the central and an offset cryoprobes

Table 3.9: Contribution of ratio of absorbed cooling power by central and offset cryoprobes.

Configuration	Initial ratio of cooling power absorbde by central probe	Initial ratio of cooling power absorbde by offset probe
1	0.58	0.42
3	0.60	0.40
5	0.61	0.49

more and decreases with respect to time finally it attains steady state, while the opposite nature is true for offset cryoperobe. The contribution to the cooling by central probe is more than the contribution to cooling power by offset cryoprobe. Initially the central cryoprobe is surrounded by offset cryoprobes, evaluation of of ice ball surrounded by central probe restricted by offset cryoprobes. This causes a high temperature gradient at the central probe compared to offset cryoprobes. This results, initially the absorbed cooling power high at the central probe and lower at offset probes, with the passage of time ice balls formed around the central and offset cryoprobes are united together and forms a single iceball. If the distance between the any of the two offset cryoprobes is more , the temperature gradient will be less and vice versa.

CHAPTER 4

Conclusion

In this study, the optimal parameters volume of ice ball around the cryoprobe, ablation ratio, cooling power requirements were predicted and compared to maximise the cell necrosis. The Percentage of increase in ice ball volume for frozen($-0.53^{O}C$) and lethal($-40^{O}C$)zones at the end of freezing process (10min) for different configuration for cryoprobe temperatures $-126^{O}C$ and -196^{0}C decreases with increase in offset cryoprobes. Ablation ratio increased by 57% for change in configuration 1 to configuration 2 at freezing time equals to 52s at cryoprobe temperature-126^{0}C, this increase is reduced to 26% for $-196^{O}C$ at 32s. similarly for configuration 5 and 6, the values are 23.76%, 16.00% at -$126^{o}C$ at 46s, 36s and 9.75%, 6.00% at$-196^{0}C$ at 30s 26s. Also, the increase in ablation ratio is found to decrease with increase in number of offset cryoprobes and ablation ratio can be achieved highly with least (configuration 1) configuration at lower cryoprobe operating temperatures. cooling power requirement increases with increase in offset cryoprobes and also increases with decrease in cryoprobe temperature. Being central probe in configuration 1 more effective than any other configuration. For configuration 1, increase in 4.5% of cooling power requirement at 52s gives the increase in ablation ratio by 57% for cryoprobe temperature equals to -126^{0}C. similarly at the same operating condition for configuration 3 increase in 1.16% of cooling power requirement, ablation ration increased by 23.76%. for configuration 5 increase in 1.45% of cooling power requirement, ablation ration increased by 16%. By increasing the number of off set cryoprobes not only increse in cooling power requirement but also decrese in ablation ratio. From this it can be concluded that the tissue necrosis maximise at the lower configuration with central probe, and significant effect of central probe can be observed with less number of offset cryoprobes only. This information can be utilised to maximise the tissue necrosis in cryosurgery.

Bibliography

[1] J. Baust, A. Gage, H. Ma, and C. M. Zhang, "Minimally invasive cryosurgery–technological advances", *Cryobiology*, vol. 34, pp. 373–384, 1997.

[2] K. J. Chua and S. K. Chou, "On the study of the freeze-thaw thermal process of a biological system", *Applied Thermal Engineering*, vol. 29, pp. 3696–3709, 2009.

[3] A. Gage and J. Baust, "Mechanisms of tissue injury in cryosurgery", *Cryobiology*, vol. 37, pp. 171–186, 1998.

[4] B. Rubinsky and G. Onik, "Cryosurgery: advances in the application of low temperatures to medicine", *International journal of refrigeration*, vol. 14, pp. 190–199, 1991.

[5] K. J. Chua, "An analytical study in the thermal effects of cryosurgery on selective cell destruction", *Journal of bioomechanics*, vol. 40, pp. 100–116, 2007.

[6] P. Mazur, "Physical-chemical factors underlying cell injury in cryosurgical freezing", In R. Rand, A. Rinfret, and H. v. Leden (eds.), *Cryosurgery*, Springfield, IL, pp. 32–51, 1968.

[7] P. Mazur, "Freezing of living cells: mechanisms and implications", *American Journal of Physiology*, vol. 247, pp. 125–142, 1984.

[8] L. keijser, "Cryosurgery of bone tumors", 2001.

[9] C. I.S, "Cryosurgery as viewed by cryosurgeon", *cryobiology*, vol. 1, pp. 44–54, 1964.

[10] P. K. G. M. I. T. J. F. E. D. F. G. M. L. Rivoire, E. J. Voiglio, "Hepatic cryosurgery precision: evaluation of ultrasonography, thermometry, and impedancemetry in a pig model", *journal of surgical oncology*, pp. 242–248, 1996.

[11] J. F. J.Smith, "An estimation of tissue damage and thermal history inthe thermal lesion", *cryobiology*, vol. 11, pp. 139–147, 1974.

[12] J. F. J. Smith and A. G. MacIver, "Ultrastructure after cryosurgery of rat liver", *cryobiology*, vol. 15, pp. 426–432, 1978.

[13] Rubinsky, "Cryosurgery", *Annual review of biomedical engineering*, vol. 2, pp. 157–187, 2000.

[14] J. Saliken, B. Donnelly, and J. Rewcastle, "The evolution and state of modern technology for prostate", *Urology*, vol. 60, pp. 26–33, 2002.

[15] A. Zisman, A. J. Pantuck, J. K. Cohen, and A. S. Belldegrun, "Prostate cryoablation using direct transperineal placement of ultrathin probes through a 17-gauge brachytherapy template – technique and preliminary results", *Urology*, vol. 58, pp. 988–993, 2001.

[16] R. Orpwood, "Biophysical and engineering aspects of cryosurgery", *Physics in medicine and biology*, vol. 26, p. 555, 1981.

[17] Z. Magalov, A. Shitzer, and D. Degani, "Experimental and numerical study of one, two, and three embedded needle cryoprobes simultaneously operated by high pressure argon gas", *Journal of Heat Transfer*, vol. 130, pp. 032301–12, 2008.

[18] J. C. Rewcastle, G. A. Sandison, L. J. Hahn, J. C. Saliken, J. G. McKinnon, and B. J. Donnelley, "A model for the time-dependent thermal distribution within an iceball surrounding a cryoprobe", *Physics in Medicine and Biology*, vol. 43, pp. 3519–3534, 1998.

[19] J. C. Rewcastle, G. A. Sandison, K. Muldrew, J. C. Saliken, and B. J. Donnelley, "A model for the time dependent three-dimensional thermal distribution within iceballs surrounding multiple cryoprobes", *Medical Physics*, vol. 28, no. 6, pp. 1125–1137, 2001.

[20] Y. Rabin and A. Shitzer, "Numerical solution of the multidimensional freezing problem during cryosurgery", *Journal of Biomechanical Engineering*, vol. 120, pp. 32–37, 1998.

[21] A. Weill and A. Shitzer, "Numerical solution of the multidimensional freezing problem during cryosurgery", *Journal of biomechanical engineering*, vol. 120, pp. 32–37, 1998.

[22] N. Shamsundar and E. Sparrow, "Analysis of multidimensional conduction phase change via the enthalpy model", *Journal of heat transfer*, vol. 97, pp. 333–340, 1975.

[23] R. G. Keanini and B. Rubinsky, "Optimization of multiprobe cryosurgery", *Journal of Heat Transfer*, vol. 114, pp. 796–801, 1992.

[24] M. Jankun, T. Kelly, A. Zaim, K. Young, R. Keck, J. K. Seifert, and J. Jankun, "Computer model for cryosurgery of prostate", *Computer aided surgery*, vol. 4, pp. 193–199, 1999.

[25] R. Baissalov, G. A. Sandison, B. J. Donnelley, J. C. Saliken, J. G. McKinnon, K. Muldrew, and J. C. Rewcastle, "A semi-empirical planning model for optimization of multiprobe cryosurgery", *Physics in Medicine and Biology*, vol. 45, pp. 1085–1098, 2000.

[26] R. Wan, Z. Liu, K. Muldrew, and J. C. Rewcastle, "A finite element model for ice ball evolution in a multiprobe cryosurgery", *Computer Methods in Biomechanics and Biomedical Engineering*, vol. 6, no. 3, pp. 197–208, 2003.

[27] N. Hoffmann and J. Bischof, "The cryobiology of cryosurgical injury", *Urology*, vol. 37, pp. 171–186, 2002.

[28] M. R. Rossi, D. Tanaka, K. Shimada, and Y. Rabin, "Computerized planning of prostate cryosurgery using variable cryoprobe", *Cryobiology*, vol. 60, pp. 71–79, 2010.

[29] Z. Zhu He, X. Xue, and J. Liu, "An effecetive finite difference method for simulation of bioheat transfer in irregular tissue", *Journal of heat transfer*, vol. 135, pp. 071003–071003, 2013.

[30] A. Kumar, "Cryosurgery of a biological tissue with multiprobe: effect of central cryoprobe", *Heat and mass transfer*, vol. 50, pp. 1751–1764, 2014.

[31] C. C. Rupp, N. E. Hoffman, F. R. Schmidlin, D. J. Swanlund, J. C. Bishof, and J. E. Coad, "Cryosurgical changes in porcine kidney: histologic analysis with thermal history correlation", *Cryobiology*, vol. 45, pp. 167–182, 2002.

[32] J. H. Ferziger and M. Peric, "Computational merthods for fluid dynamics", *Springer*, vol. 3, 2002.

[33] V. R. Voller and C. Prakash, "A fixed grid numerical modelling methodology for convection-diffusion mushy-region phase change problems", *International Journal of Heat and Mass Transfer*, vol. 30, no. 8, pp. 1709–1719, 1987.

[34] S. Kakac and Y. Yener, *Heat conduction*, Hemisphere publishing corporation, 1985.

[35] A. Kumar and S. Roy, “Heat transfer charecterstics during melting of a metal spherical particle in its own liquid”, *International journal of Thermal science*, vol. 49, pp. 397–408, 2009.

[36] A. Bejan and K. AD, *Heat transfer hand book*, John wiley and sons Newyork, 2003.